River ecomorphodynamics and bioengineering

(ENV-418, A.Y. 2025-26)

4ETCS, Master option

Prof. Paolo Perona
Platform of Hydraulic Constructions

Lecture 12-2: Plant effects on hydraulic resitance to flow, root biomechanics

Salicacee and fluvial processes

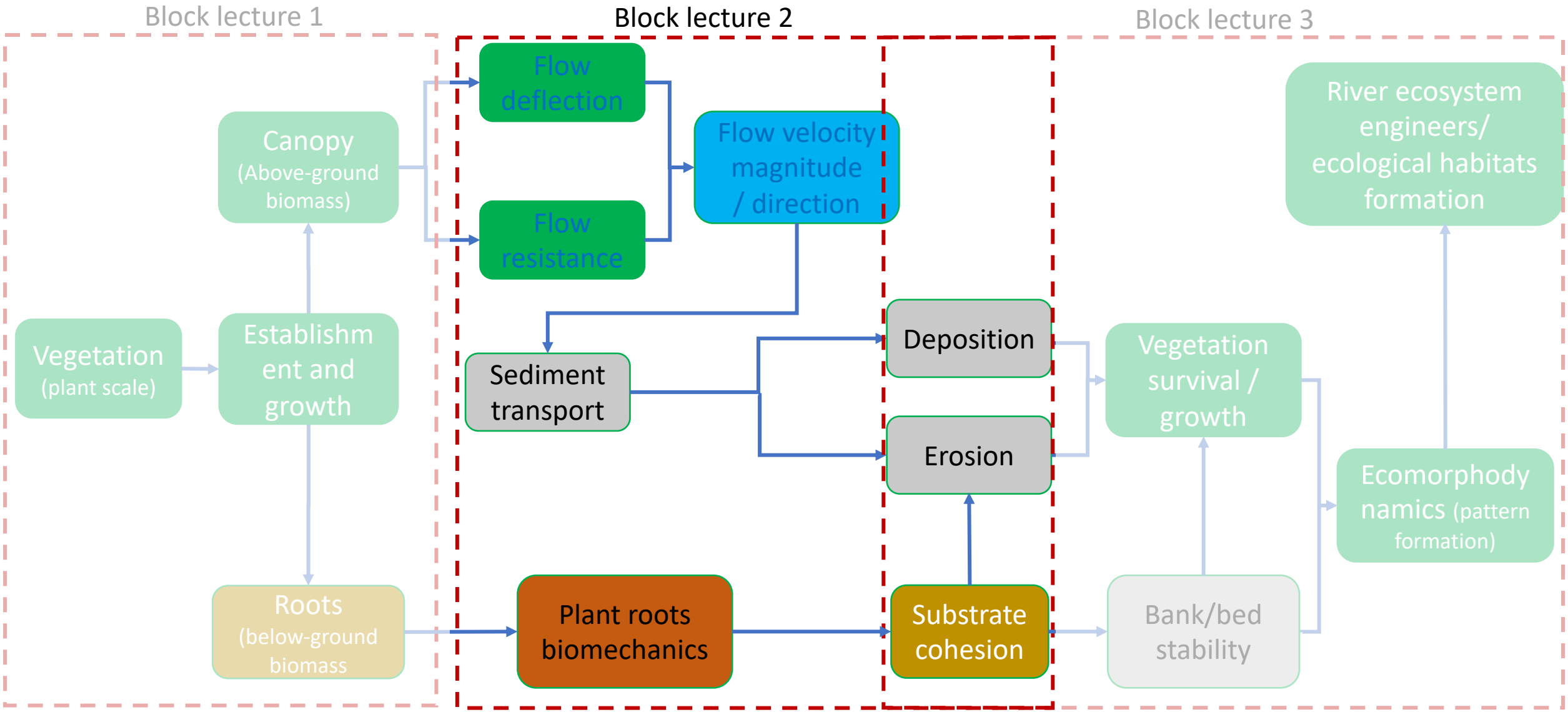

Hydraulic role and resistance to flow of plants and vegetated patches

Flow resistance

Single plant

- Flexibility
- Foliation

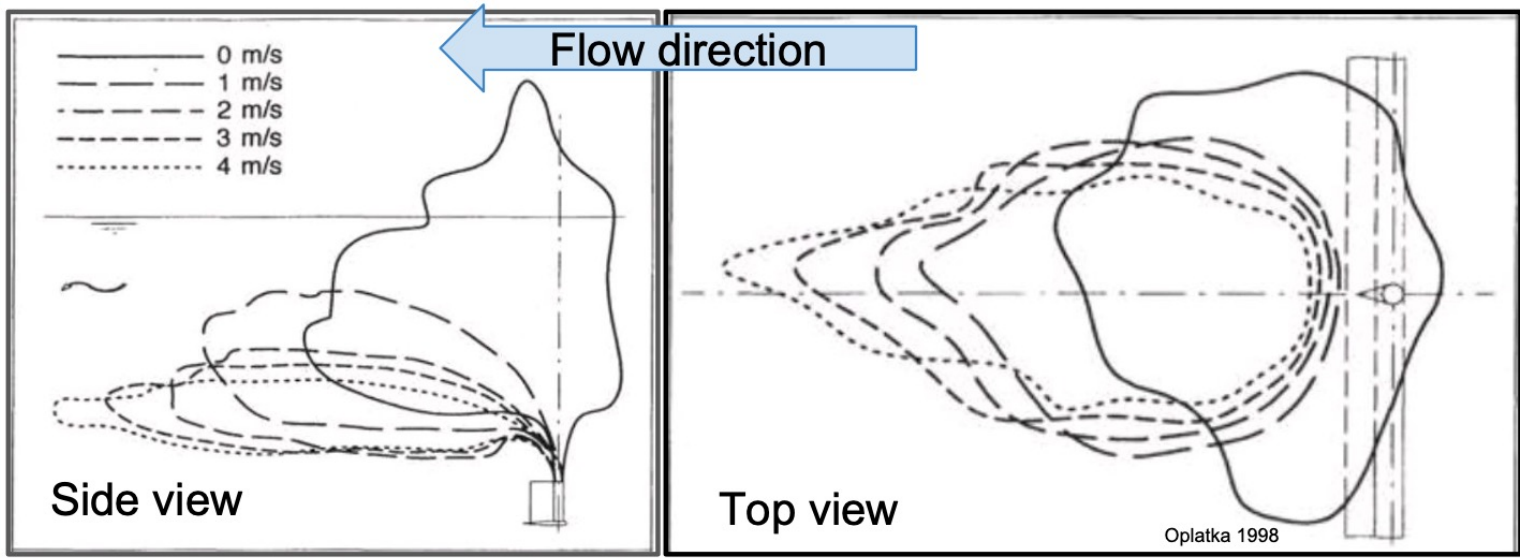

Patch scale

- Plant density

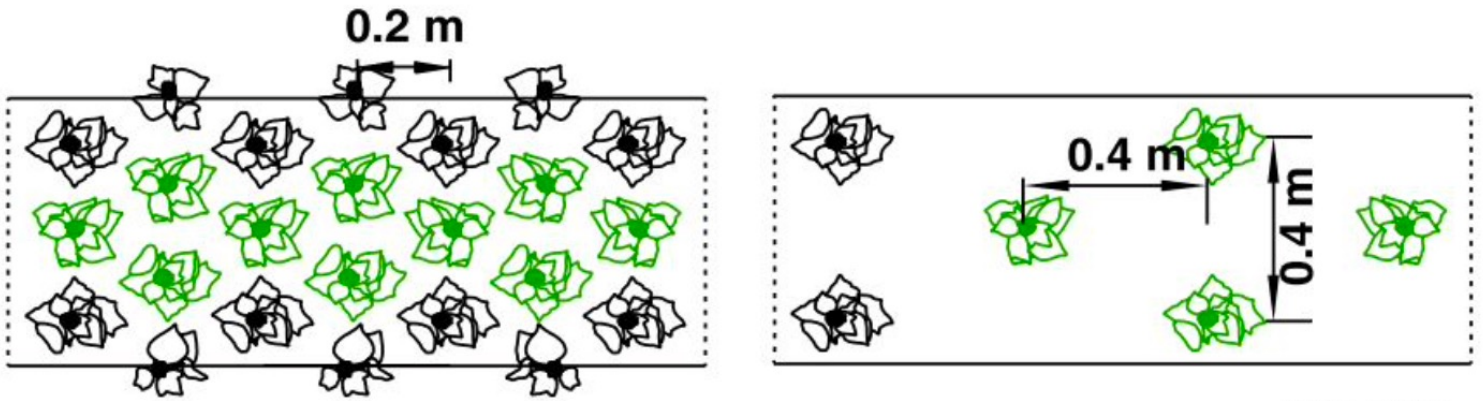

Jalonene et al 2013

Oplatka, Matthias. “Stabilitaet von Weidenverbauungen an Flussurfen.” Technischen Hochschule Zuerich, 1998

Jalonen, J., J. Järvelä, and J. Aberle. “Leaf Area Index as Vegetation Density Measure for Hydraulic Analyses.” Journal of Hydraulic Engineering 139, no. 5 (2013): 461–69. .

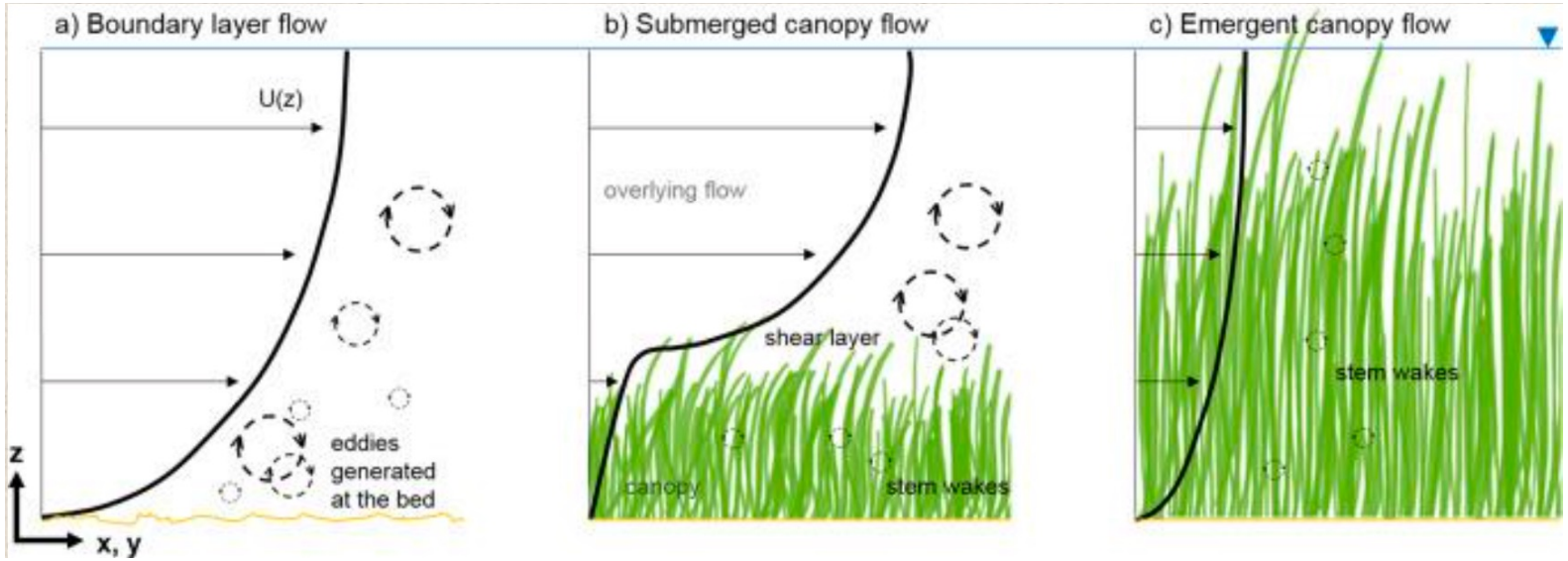

Q=30 m³/s

Q=500 m³/s

Type of flow-canopy interaction

- Submerged vegetation
  - Rigid
  - Flexible
- Emerged vegetation
  - Rigid
  - Flexible

Flow structure for emergent non-porous obstacles

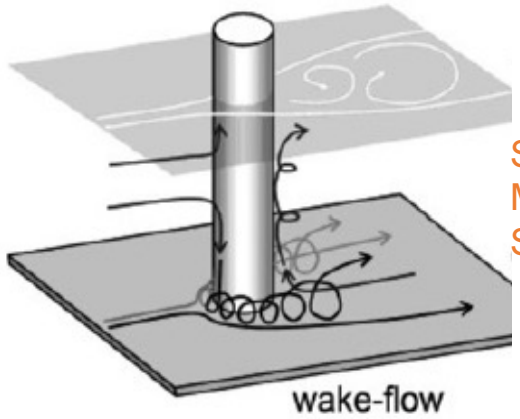

Figure 1. Schematized types of flow around tall vegetation.

Schnauder & Moggridge, Aq. Sci. 2009

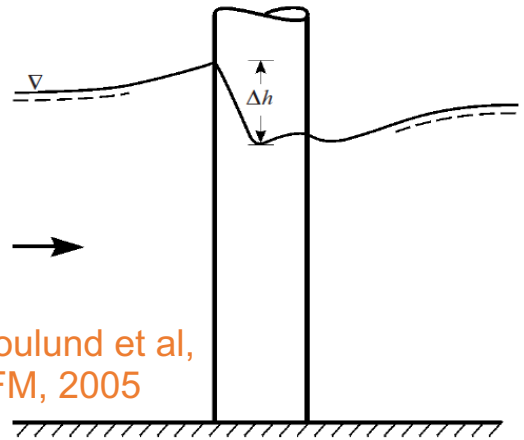

Roulund et al, JFM, 2005

Bed shear stress

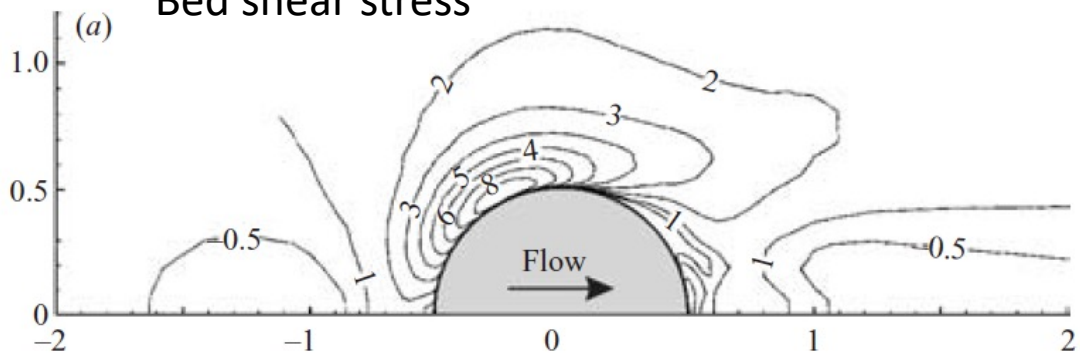

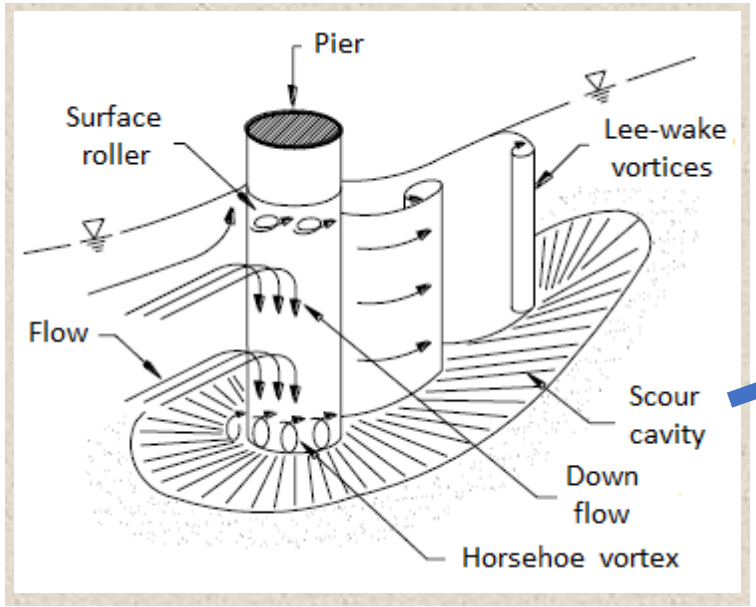

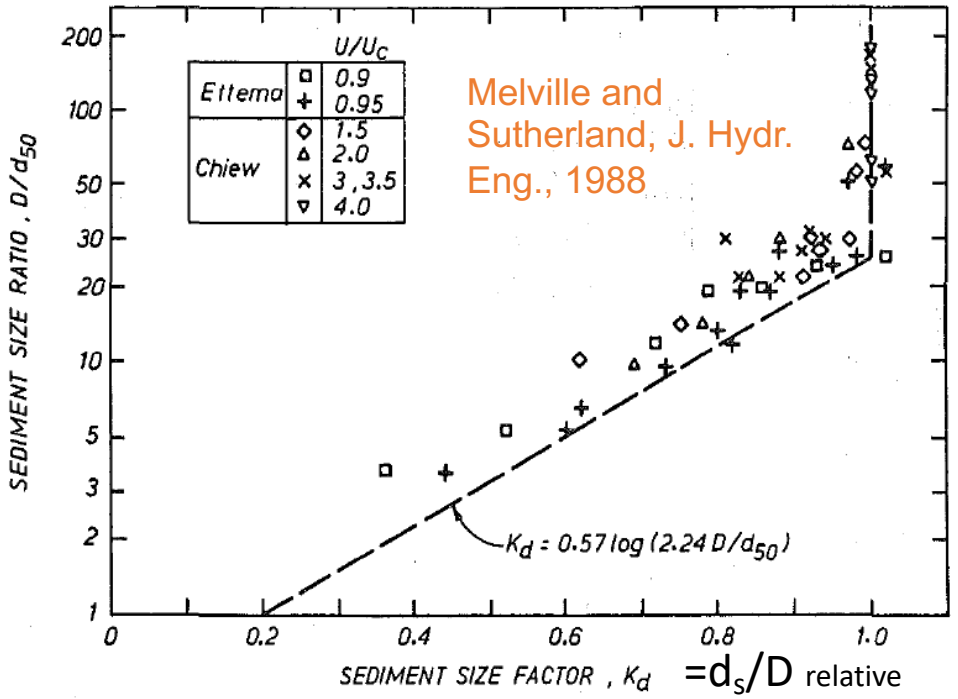

FIG. 4. Influence of Sediment Size on Scour Depth

1D steady flow: deep layer approximation (US Corp of Eng)

Resistance to flow is typically characterized by a roughness coefficient. The most commonly used equation for flow resistance is the Manning's equation:

$$V = \frac{K_n}{\mathrm{n}} R_h^{2/3} S^{1/2}$$

where

V = mean velocity of flow

R_h = hydraulic radius

S = slope of the energy grade

n = Manning's resistance coefficient

K_n = unit correction factor of 1.0 for SI units and 1.486 for non-SI units

Although Manning's equation is used extensively for calculating flow resistance, Manning himself did not recommend it for use, because his research found that n was not constant but varied with velocity and depth.

$$(1) \qquad \frac{V_*}{V} = \frac{\sqrt{gR_hS}}{V} = \left(\frac{\tau_o}{\rho V^2}\right)^{1/2}$$

$$\frac{V_*}{V} = \sqrt{\frac{f}{8}} = \frac{n}{K_n}\sqrt{\frac{g}{R_h^{1/3}}} = \frac{\sqrt{g}}{C}$$

$$\mathrm{n} = (\mathrm{n_o} + \mathrm{n_1} + \mathrm{n_2} + \mathrm{n_3} + \mathrm{n_4})m$$

$$\mathrm{n} = \frac{PR_h^{5/3}}{\sum_{i=1}^{N}\left(\frac{P_i R_{hi}^{5/3}}{n_i}\right)}$$

P is the wetted perimeter. N is the number of i subsections.

n=0.11

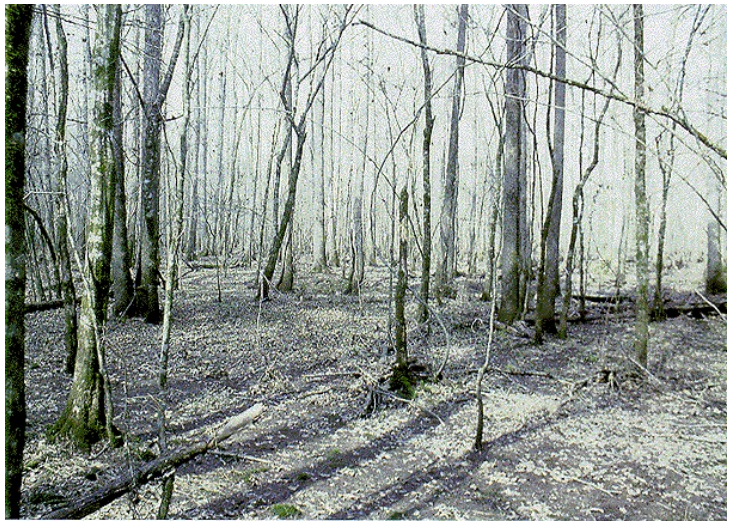

n=0.13

n=0.14

n=0.15

n=0.18

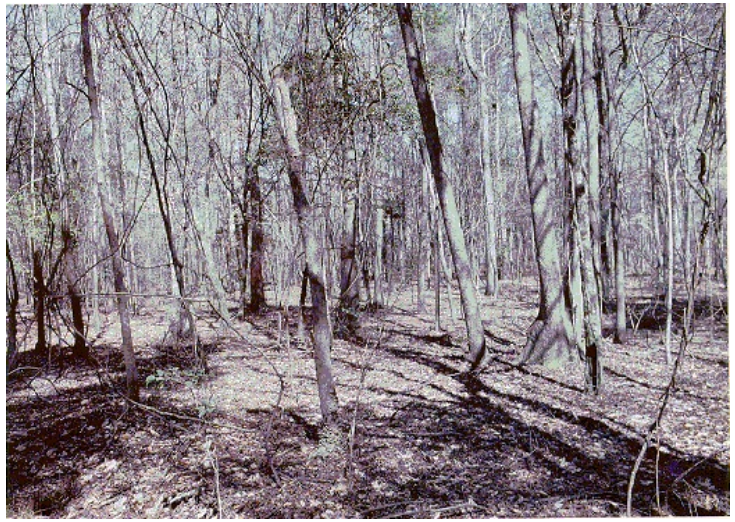

n=0.20

Flow structure for submerged canopy

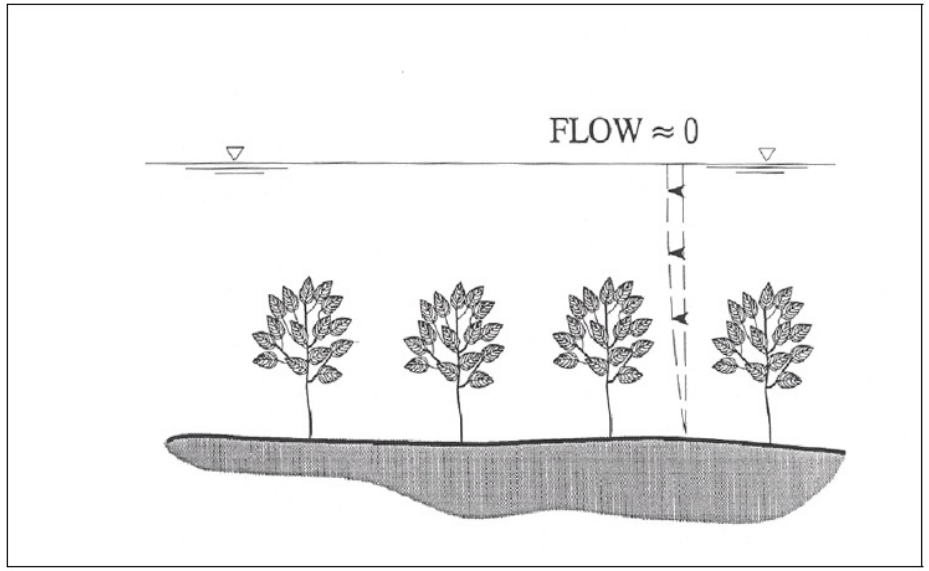

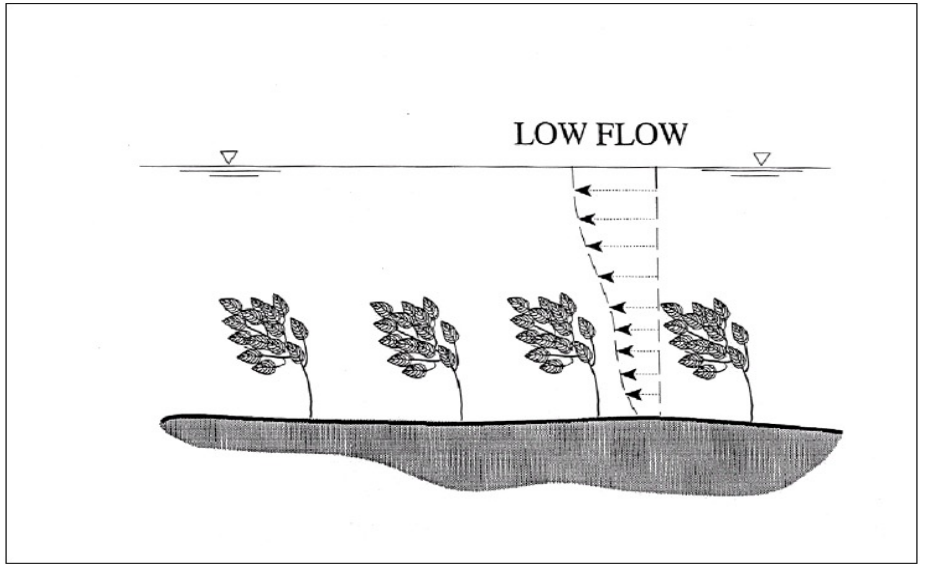

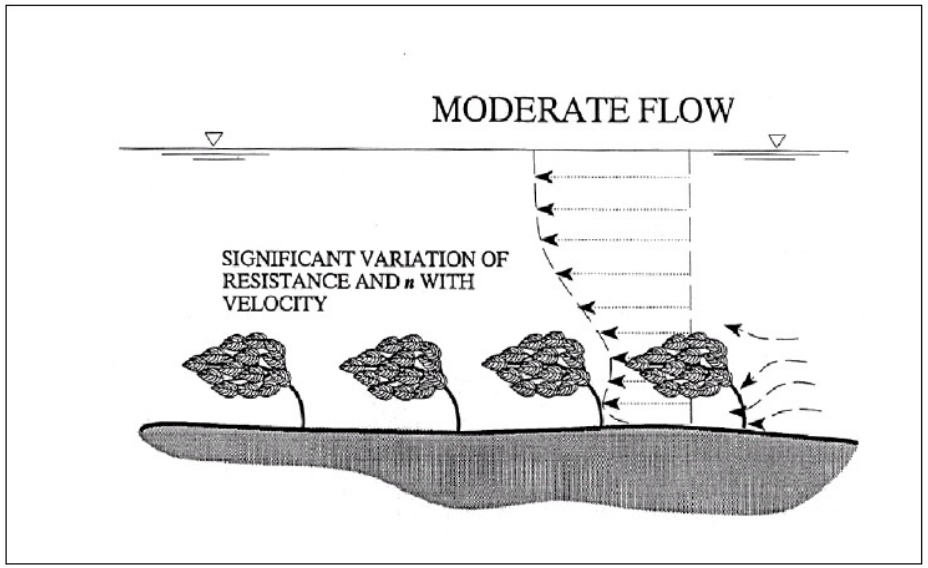

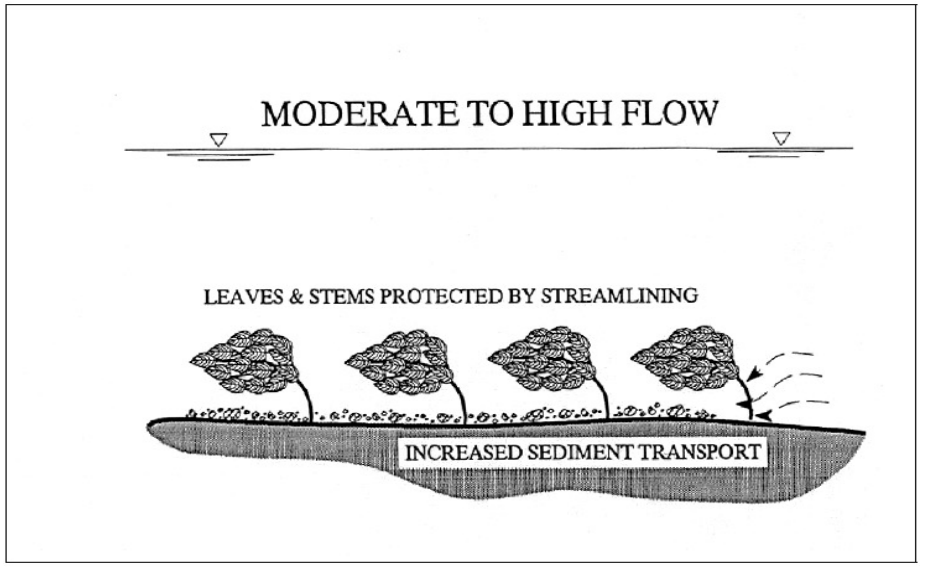

The velocity profile can be substantially modified by the presence of the canopy.

Part of the Turbulent Kintic Energy (TKE) is absorbed by vegetation

New flow structure originate by the coupling of fluctuating plants and flow vortexes (instabilities)

1D Physical approach to shallow vs deep layer approximation

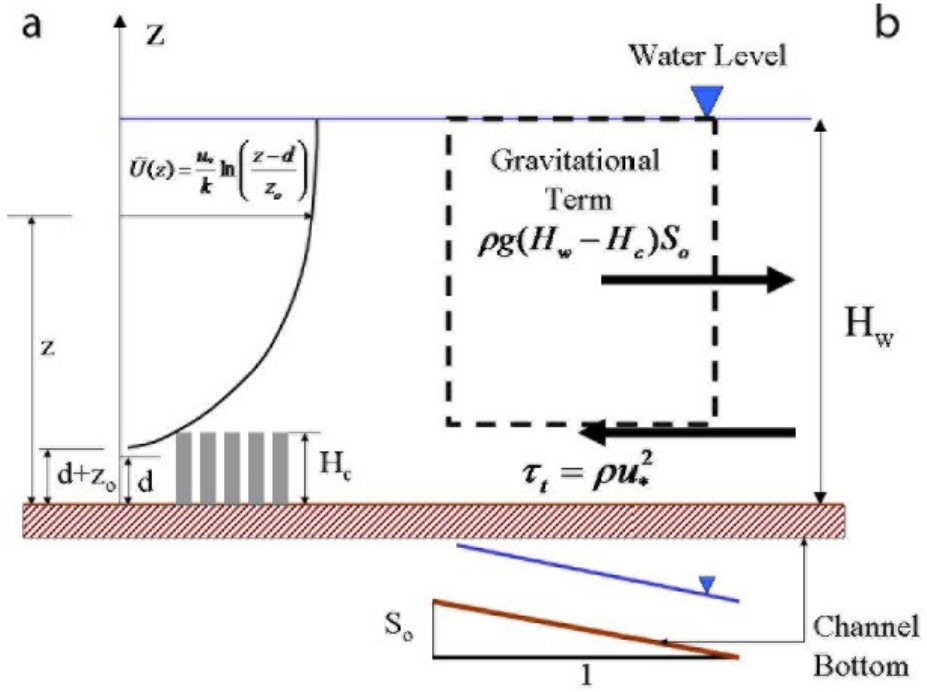

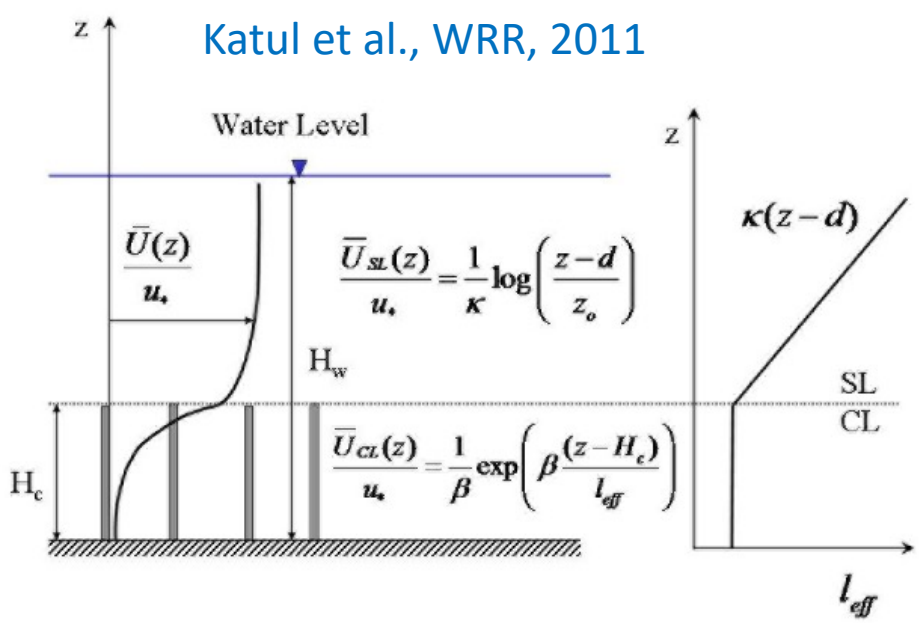

Katul et al., WRR, 2011

Deep Layer Approximation: $H_w >> H_c$

$$\sqrt{\frac{f}{8}}=\left(\frac{2\kappa e^{1/7}}{5}\right)\left(\frac{z_o}{H_w}\right)^{1/7}\approx 0.18\left(\frac{z_o}{H_w}\right)^{1/7}.$$

$$n=\left(\kappa/\sqrt{g}\right)H_w^{1/6}\left[\ln(H_w/z_o)-1\right]^{-1}$$

Shallow Layer Approximation: $H_w \approx H_c$

$$\frac{U_b}{u_*}=\sqrt{\frac{8}{f}}=\frac{H_w^{1/6}}{n\sqrt{g}}=\overbrace{2\beta\frac{L_c}{H_w}\left[1-\exp\left(-\frac{1}{2\beta^2}\frac{H_c}{L_c}\right)\right]}^{\text{Direct Canopy Layer Effects}}+\frac{1}{2}$$

$$\underbrace{\frac{1}{\kappa}\left(1-\frac{H_c}{H_w}\right)\left\{-1+\ln\left[\left(\frac{H_w-d}{z_o}\right)^{(H_w-d)/(H_w-H_c)}\left(\frac{H_c-d}{z_o}\right)^{-(H_c-d)/(H_w-H_c)}\right]\right\}}_{\text{Perturbed Log. Profile Due to Canopy Layer Effects}}.$$

Other models of vegetation roughness

$$C_{r\,vV} = \frac{h_v u_{v\,vV} + (h - h_v) u_{s\,vV}}{h\sqrt{hi_b}}$$

$$C_{r\,B} = \sqrt{\frac{1}{\frac{1}{C_b^2} + \frac{C_D a h_v}{2g}} + \frac{\sqrt{g}}{\kappa} \ln\left(\frac{h}{h_v}\right)}$$

$$C_{r\,P\&B} = \sqrt{\frac{2g}{ahC_D}}$$

$$C_{r\,J} = \sqrt{1-\lambda}\, C_{r\,P\&B} = \sqrt{\frac{2g(1-\lambda)}{ahC_D}}$$

$$C_{r\,Y\&C} = \sqrt{\frac{2g}{ah_v C_D}} + \frac{C_u}{\kappa}\sqrt{g\left(1-\frac{h_v}{h}\right)}\left[\ln\left(\frac{h}{h_v}\right) - \left(1-\frac{h_v}{h}\right)\right]$$

$$C_{r\,Hof} = \sqrt{h - \frac{\pi D2}{2s_{Hof}}}\, C_{r\,P\&B} = \sqrt{\frac{2g}{ahC_D}\left(h - \frac{\pi D^2}{2s_{Hof}}\right)}$$

$$C_{r\,S\&S} = 1.385\left(\frac{h}{h_v} - D\sqrt{m}\right)\sqrt{\frac{g}{ah}}$$

$$C_{r\,K} = h^{\frac{-3}{2}}\left\{\begin{array}{l} \frac{2}{A}(B_1 - B_2) + \frac{u_{v0}}{A}\ln\left[\frac{(B_1 - u_{v0})(B_2 + u_{v0})}{(B_1 + u_{v0})(B_2 - u_{v0})}\right] + \\ \frac{\sqrt{gB_3}}{\kappa}\left[B_3\ln\left(\frac{B_3}{k_P}\right) - h_s\ln\left(\frac{h_s}{k_P}\right) - (h - h_v)\right] \end{array}\right\}$$

Degree of submergence!

$$C_{L\&N} = \left(\frac{2}{C_f}\right)^{1/2}\left(1 - \frac{h_v}{Y}\right)^{3/2} + \left(\frac{2}{C_D\,\phi\,h_v\,D_v\,\phi_m}\right)^{1/2}\frac{h_v}{Y}$$

$$C_{r\,Ch} = (1-\lambda)\sqrt{\frac{2gr_v}{h_v C_D}}\left(\frac{h_v}{h}\right)^{\frac{3}{2}} + 4.54\sqrt{g}\left[\left(\frac{1}{\lambda} - 1\right)\left(\frac{h - h_v}{D}\right)\right]^{\frac{1}{16}}\left(1 - \frac{h_v}{h}\right)^{\frac{3}{2}}$$

P&B: Petryk and Bosmajian (1975)
J: James et al. (2004)
Hof: Hoffmann (2004)
K: Klopstra et al. (1997)
vV: van Velzen et al. (2003)
H: Huthoff (2007)
Y&C: Yang and Choi (2010)
S&S: Stone and Shen (2002)
B: Baptist et al. (2005)
Ch: Cheng (2011)
L&N: Luhar and Nepf (2014)

Effects of the canopy (porous obstacle) on transport processes

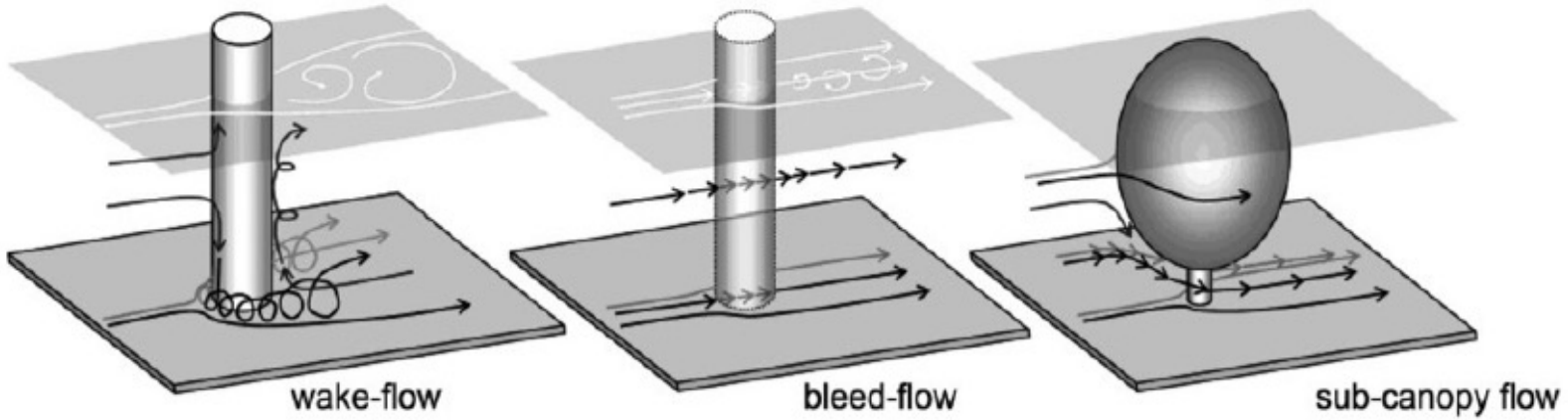

Figure 1. Schematized types of flow around tall vegetation.

Schnauder & Moggridge, Aq. Sci. 2009

The interaction between flow and the above-ground biomass in rivers is responsible for enhanced either erosion or deposition of sediment, depending on obstacle porosity (very much studied)

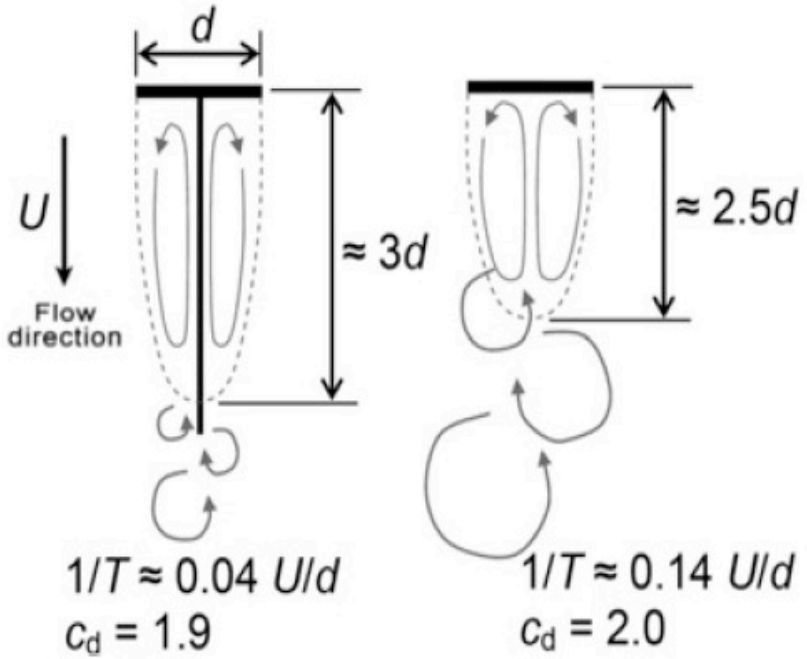

Flow deflection

Planar view

Side view

Finite width patch

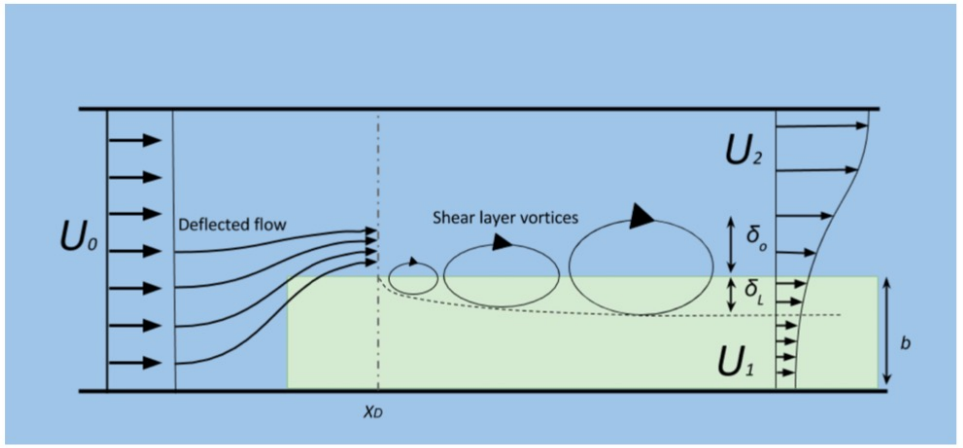

Partially submerged

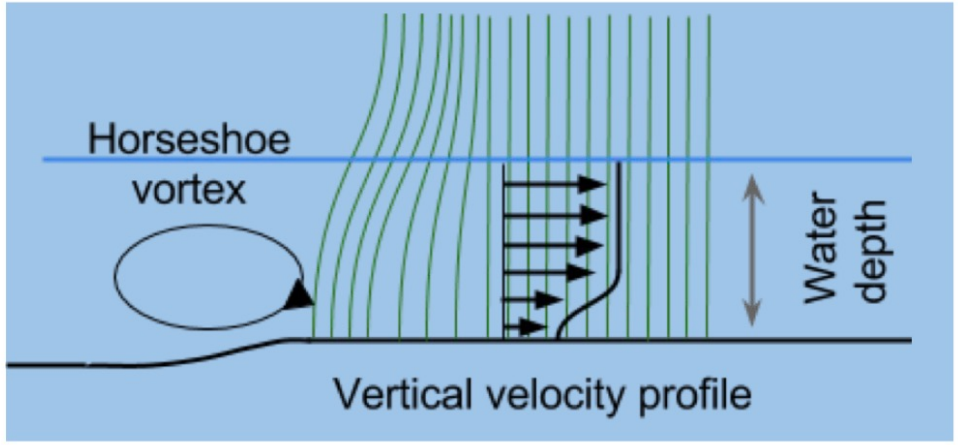

Circular patch

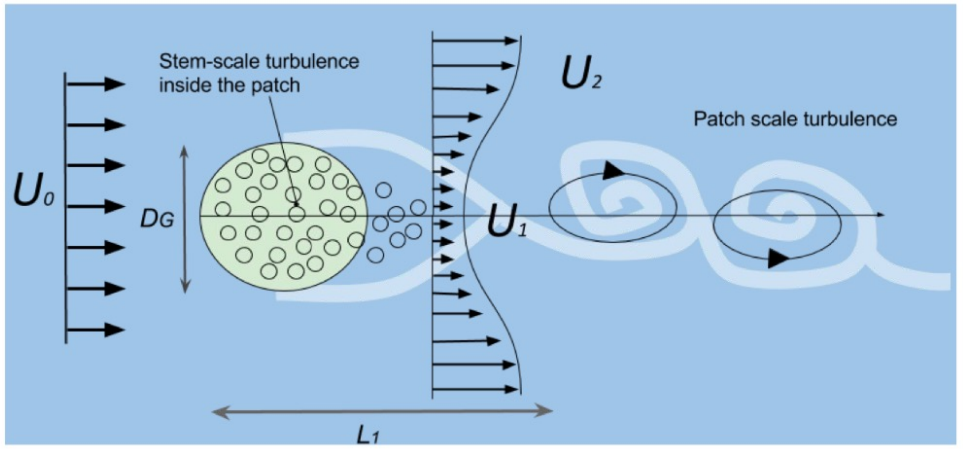

Submerged

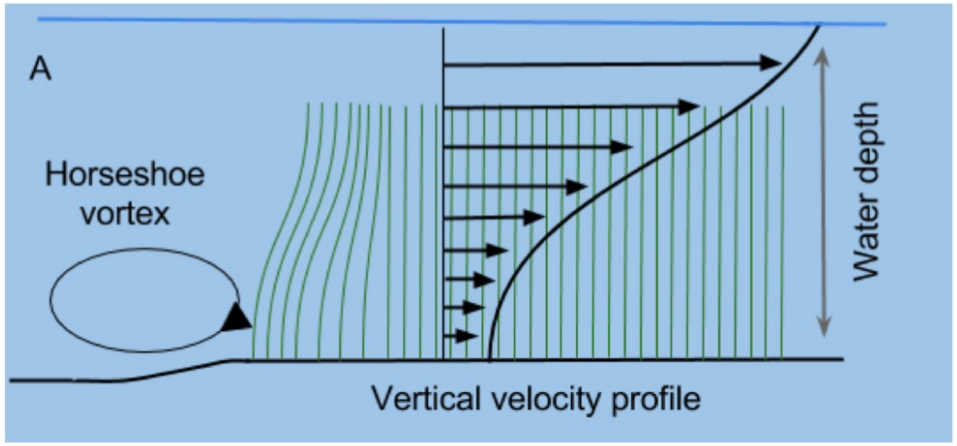

Slide courtesy of E. Politti

Politti, E., Bertoldi, W., Gurnell, A.M., Henshaw, A., 2017. Feedbacks between the riparian Salicaceae and hydrogeomorphic processes: A quantitative review. Earth-Science Rev. doi:10.1016/j.earscirev.2017.07.018

PLATEFORME DE CONSTRUCTIONS HYDRAULIQUES

Plant root biomechanics:
resistance to (static) uprooting and critical rooting length

EPFL

Mechanical resistance to uprooting

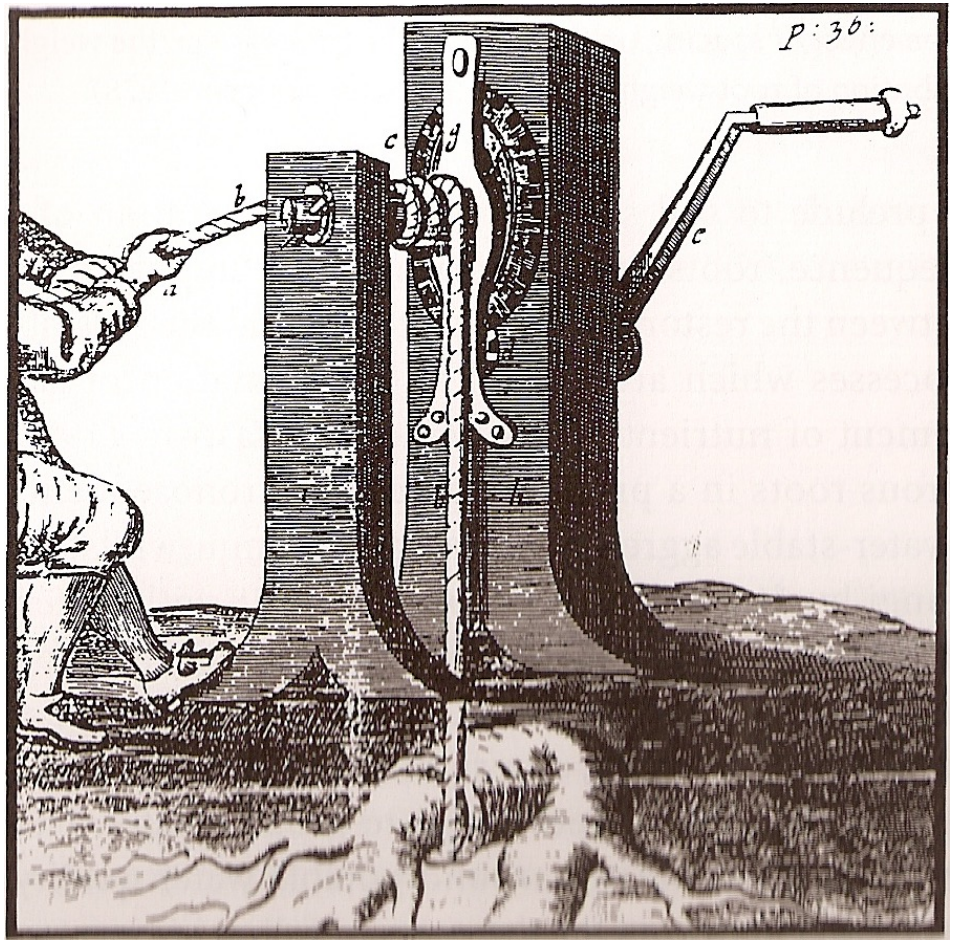

An early publication of Evelyn (1662) indicates a method to extract roots for use as an energy source, firewood (cited in Smit, 2000).

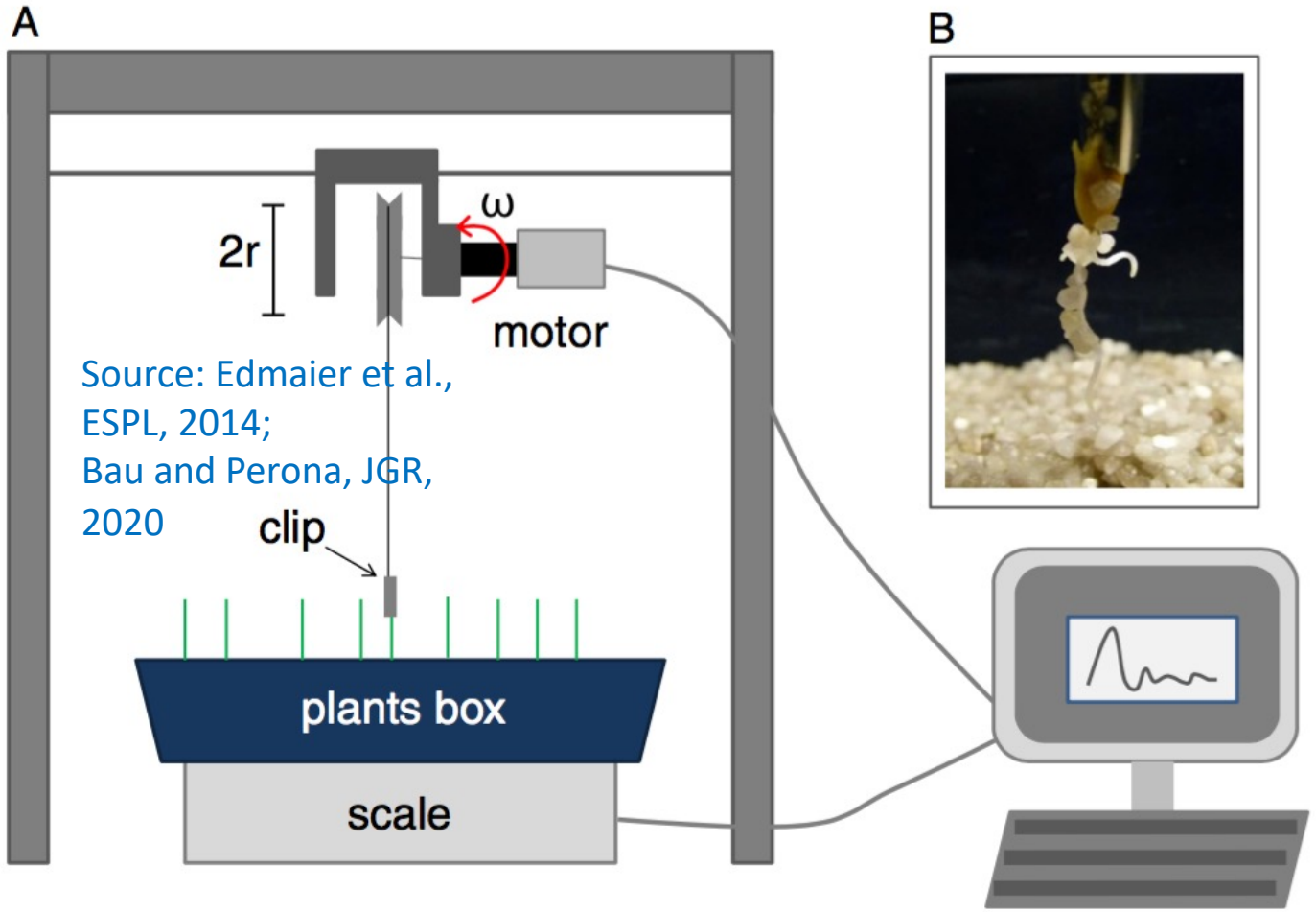

Source: Edmaier et al., ESPL, 2014; Bau and Perona, JGR, 2020

Many experiments have also been done at the field scale (Ennos, J. Theor. Biol. 1993, Pollen and Simon, 2005, Schwarz et al., 2010)

Force – displacement relationship for rooted systems

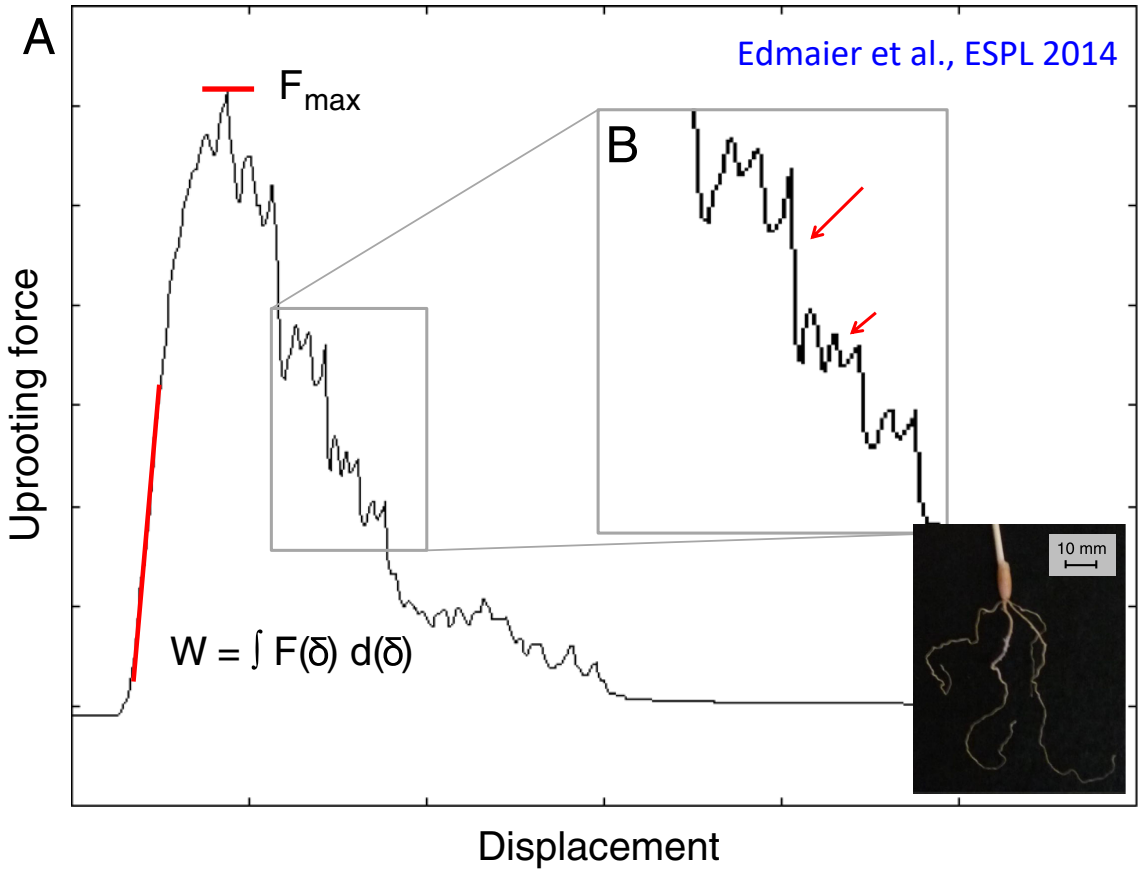

Crouzy et al., JTB, 2014

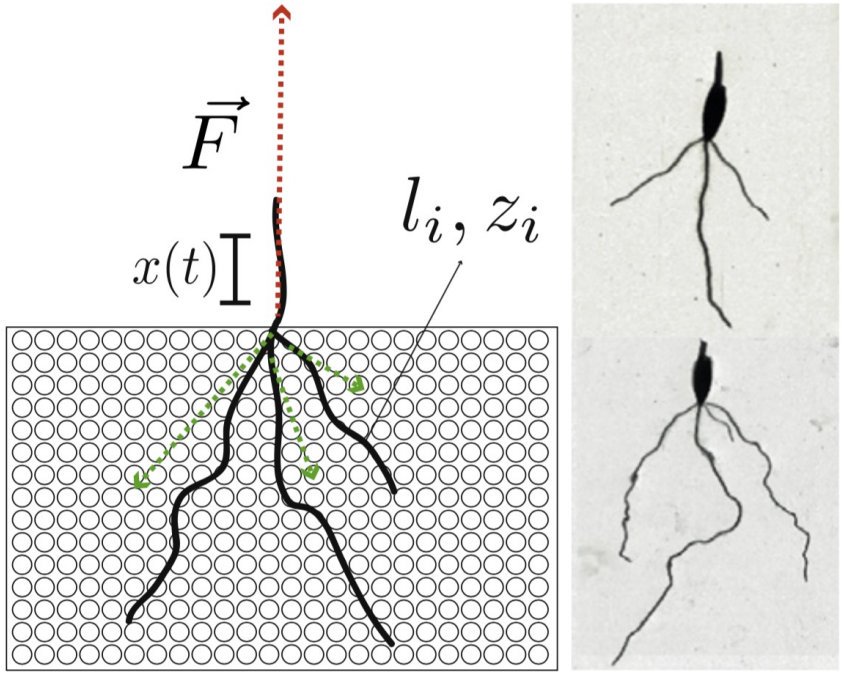

Force–displacement curve of a seedling of Avena sativa with a total root length of 132 mm and three roots. The red line in panel A indicates the linear component of the uprooting process, resulting from both elastic deformation of the root and the sediment. Arrows in panel B indicate force drops due to root release from the sediment (more pronounced) or sediment movement (less pronounced).

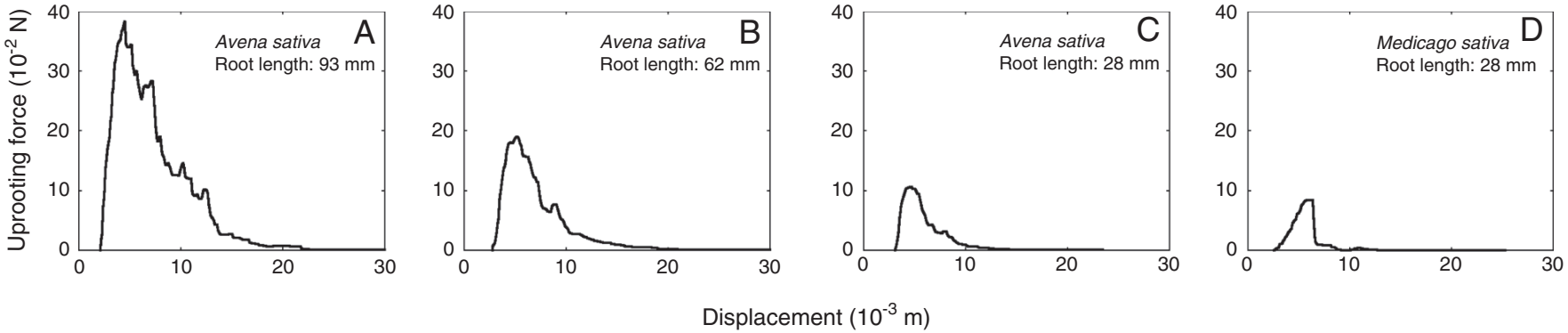

Force–displacement curves for plants of *Avena sativa* (A)–(C) and *Medicago sativa* (D) with varying root length

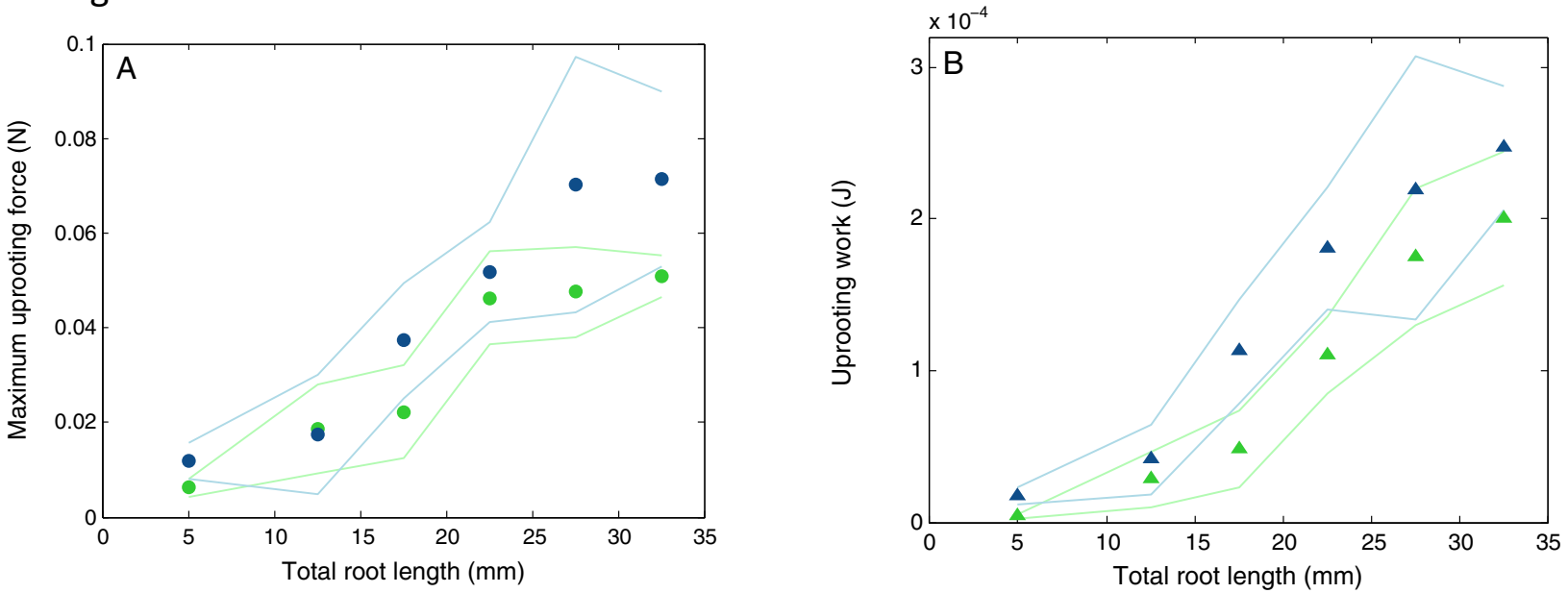

Maximum uprooting force (A) and uprooting work (B) for Avena sativa (blue) and Medicago sativa (green). Markers indicate average values for adjacent root length classes and are placed at the middle of the respective class. Light coloured lines indicate standard deviations for the respective root length class.

Avena sativa (multiroot system)

Medicago sativa (single root system)

Edmaier et al., ESPL 2014

Max force vs uprooting energy

$Q = CR^a$

Force (N)

0.0052 I_{tot}
0.0048; 0.0056
$R^2 = 0.76$
0.0034 I_{tot}
0.0030; 0.0038
$R^2 = 0.76$
0.0036 I_{tot}
0.0032; 0.0040
$R^2 = 0.78$

a=1

0.0027 I_{tot}
0.0025; 0.0029
$R^2 = 0.52$
0.0021 I_{tot}
0.0019; 0.0023
$R^2 = 0.40$
0.0019 I_{tot}
0.0017; 0.0021
$R^2 = 0.35$

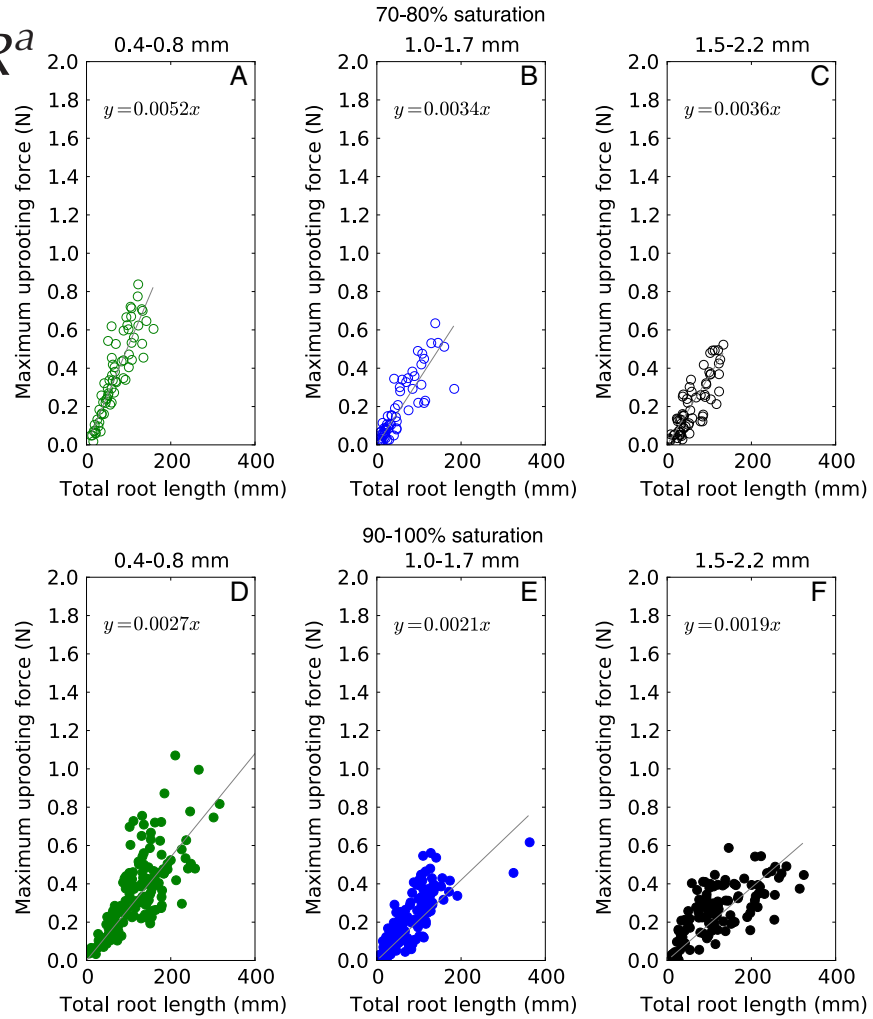

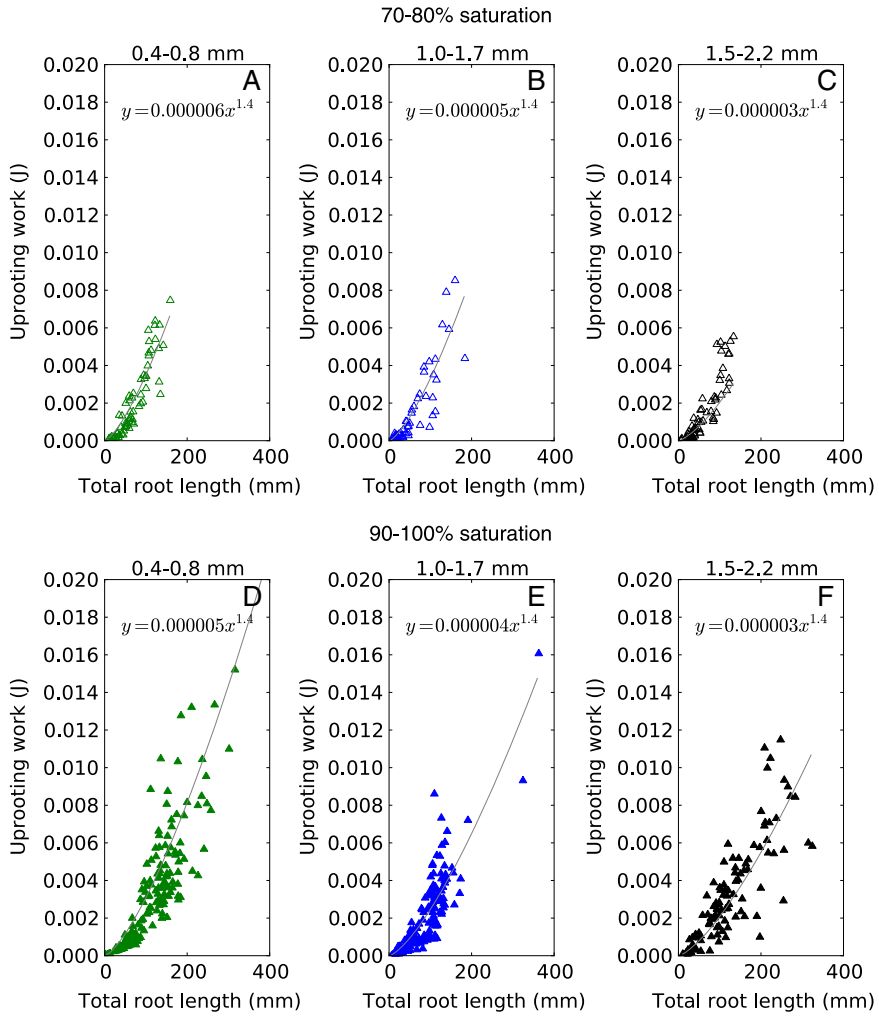

$Q = CR^a$

Work (J)

5.6 10^{-6} $I_{tot}^{1.4}$
4.8 10^{-6}; 5.9 10^{-6}

4.9 10^{-6} $I_{tot}^{1.4}$
4.3 10^{-6}; 5.5 10^{-6}

5.3 10^{-6} $I_{tot}^{1.4}$
4.6 10^{-6}; 5.9 10^{-6}

a=1.4

3.9 10^{-6} $I_{tot}^{1.4}$
3.6 10^{-6}; 4.2 10^{-6}

3.2 10^{-6} $I_{tot}^{1.4}$
3.0 10^{-6}; 3.5 10^{-6}

3.3 10^{-6} $I_{tot}^{1.4}$
3.0 10^{-6}; 3.6 10^{-6}

Ennos (1993)
a~1.5

Mechanical model (minimalist)

Crouzy et al., JTB, 2014

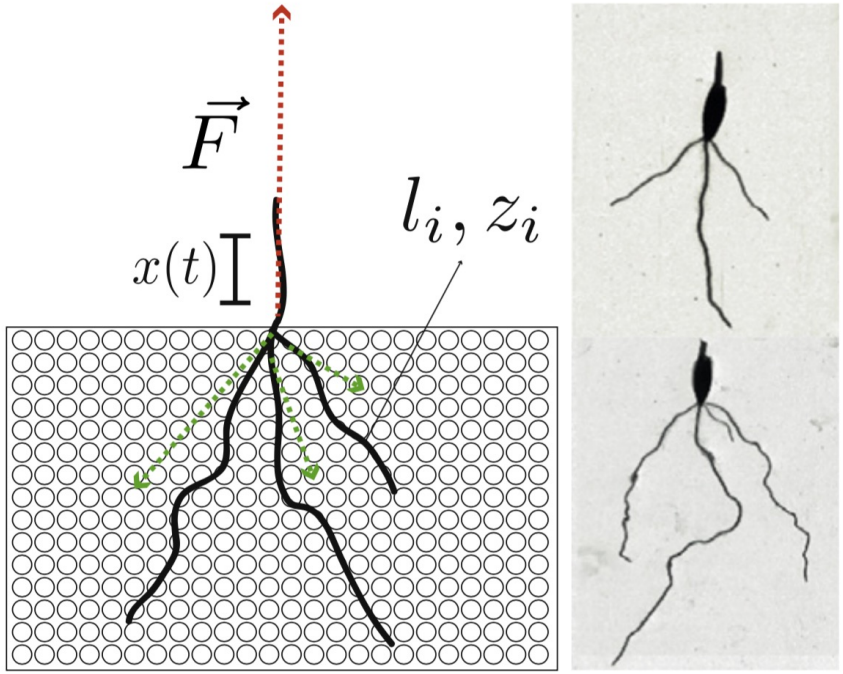

$$F_e(t) = \frac{EA}{l}(x(t) - z(t)),$$

$$F_{f_{0,d}} = f_{0,d}\pi d_r(l - z(t)).$$

$$\frac{dz}{dx} = \Theta(F_e - F_{f_0 f_d}),$$

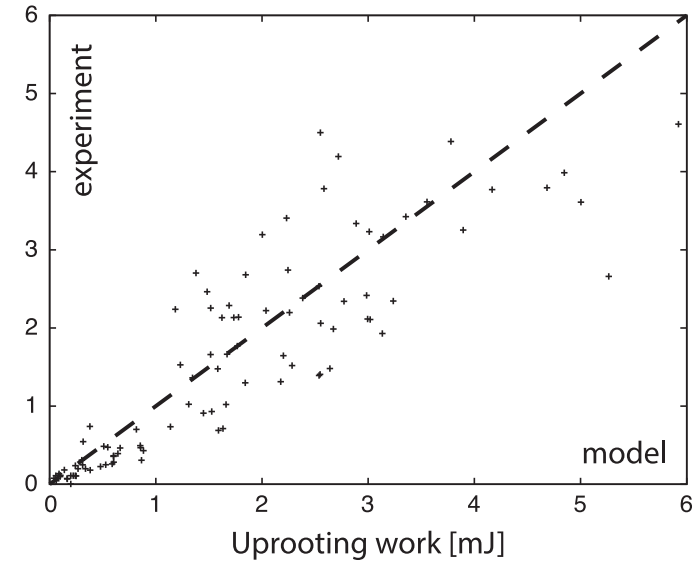

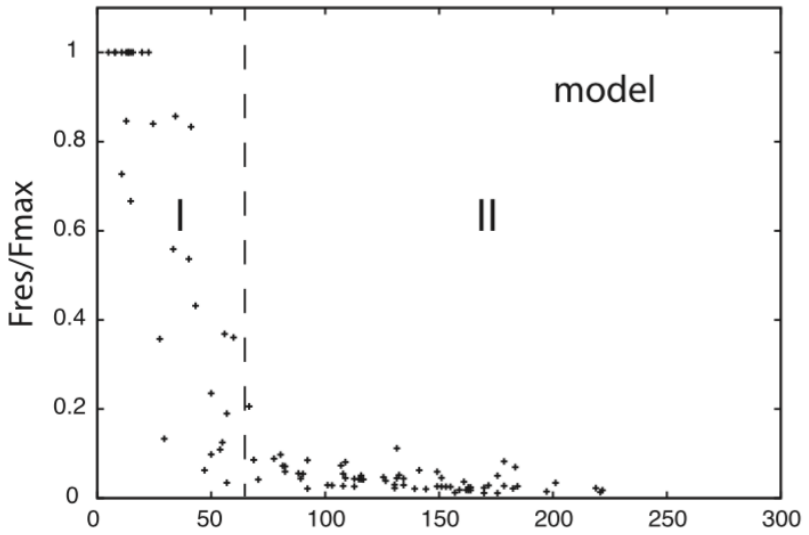

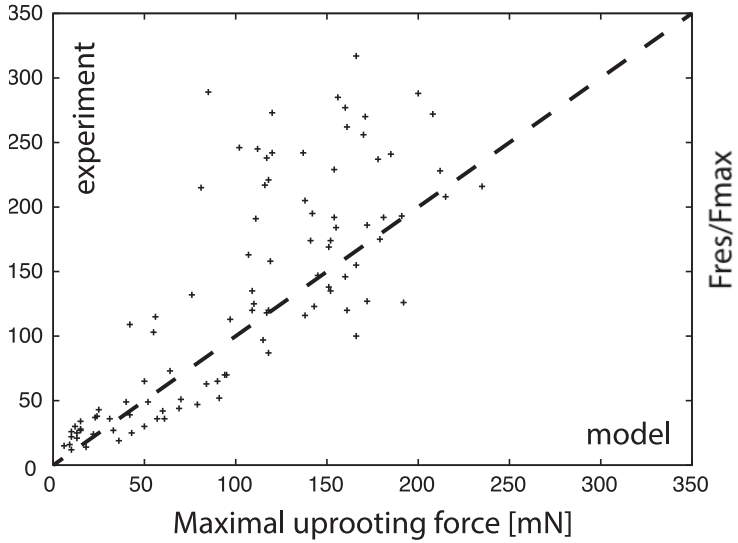

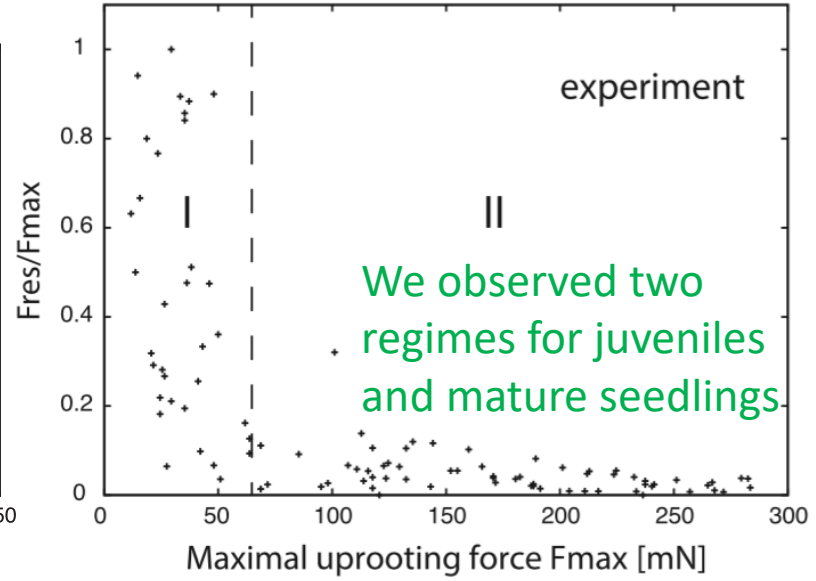

We observed two regimes for juveniles and mature seedlings

Conclusions from lab experiments

1. Maximum uprooting force and work correlate differently with total root length, and number of roots, because roots are expected to work and fail progressively.

collaboration of individual roots sums to give the uprooting work of the whole root system (Bailey et al., 2002)

2. Sediment characteristics influence uprooting resistance, with finer sediment leading to larger uprooting forces (Dupuy et al., 2005)

Anchorage will be stronger for seedlings grown in finer sediment because of larger contact area.

3. Uprooting of seedlings will require greater force at lower levels of sediment moisture (Ennos, 1990; Schwarz et al, 2011).

Full sediment saturation would reduce the ability of a seedling to withstand uprooting.

The chance of flood survival for riparian seedlings should be higher when they grow on fine sediment. Resilience to flow duration (i.e. work depends on N roots) is a better strategy than resistance to peak flow (i.e., max force does not depend on N roots)

Uprooting of seedlings in the field

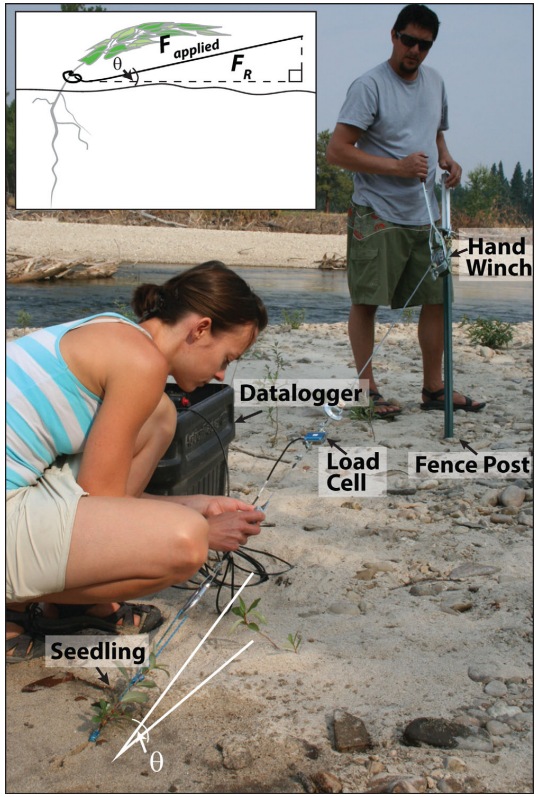

From Bywater-Reyes et al., 2015

Table 2. Sample Sizes (n) for Seedling Pull Tests and Excavations[a]

Experiment Type	Populus	Tamarix
	BR	
Scour Depth (m)		
0	83	NA
0.1	34	NA
0.2	33	NA
0.3	34	NA
0.4	13	NA
Excavated	34	NA
	BWR	
Scour Depth (m)		
0	39	34
0.2	8	8
Excavated	1	6
	SMR	
Scour Depth (m)		
0	28	28
0.2	15	6
0.3	6	5
Excavated	5	4

[a]Pull tests were conducted for different scour depths, and a subset of seedlings were excavated (supporting information Data Set S1).

a) No basal scour;
b) Basal scour

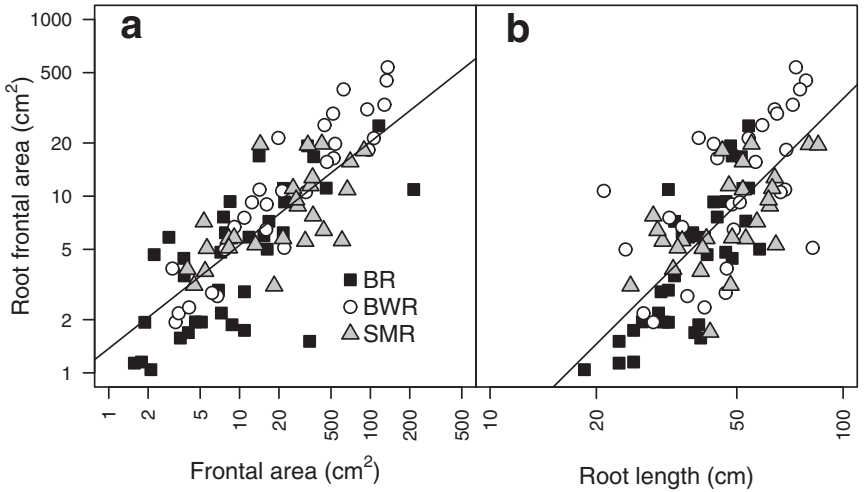

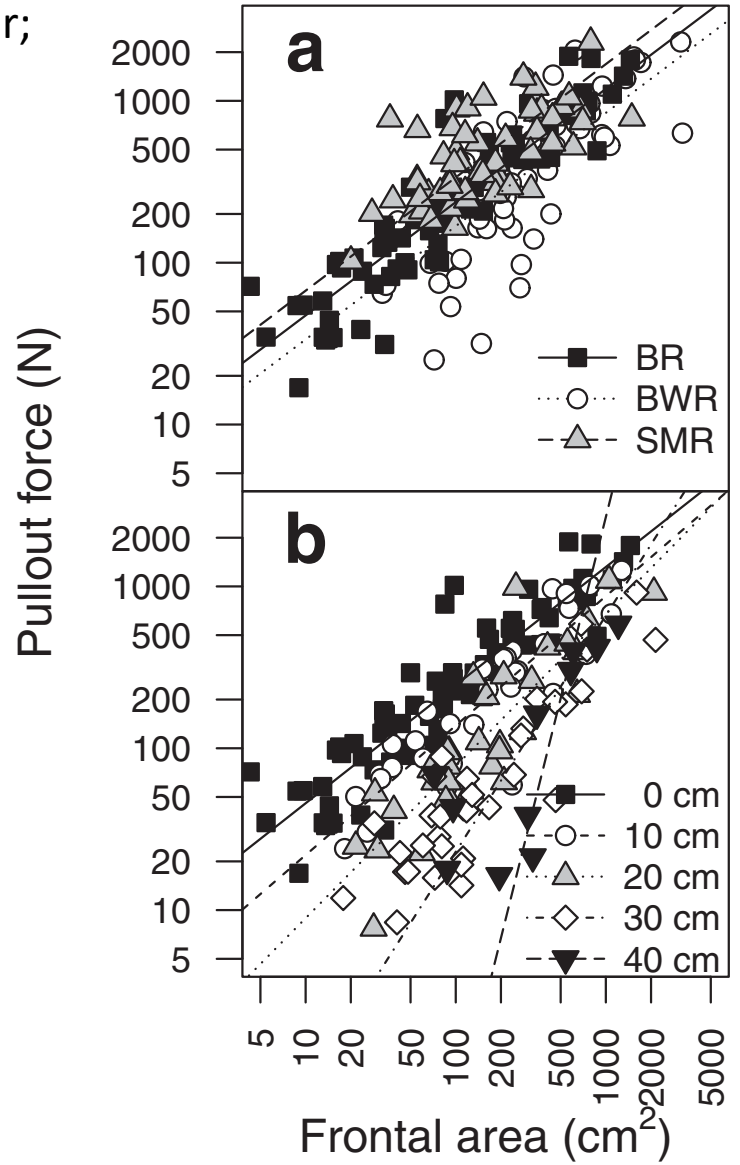

Pullout force vs plastic bending

Pullout

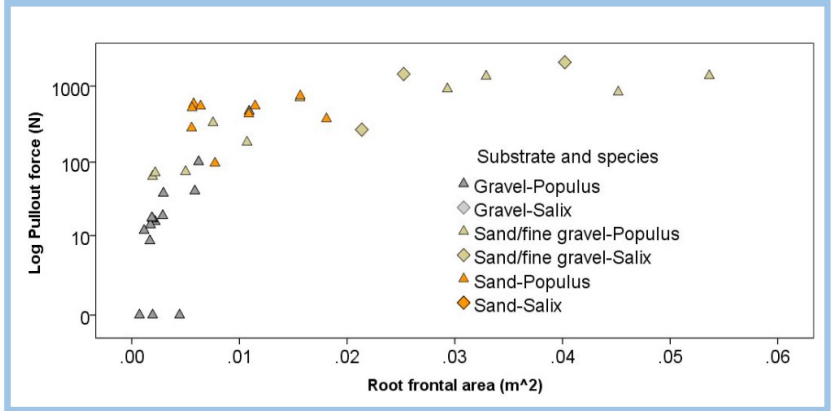

Plastic Bending - Trunk Breakage

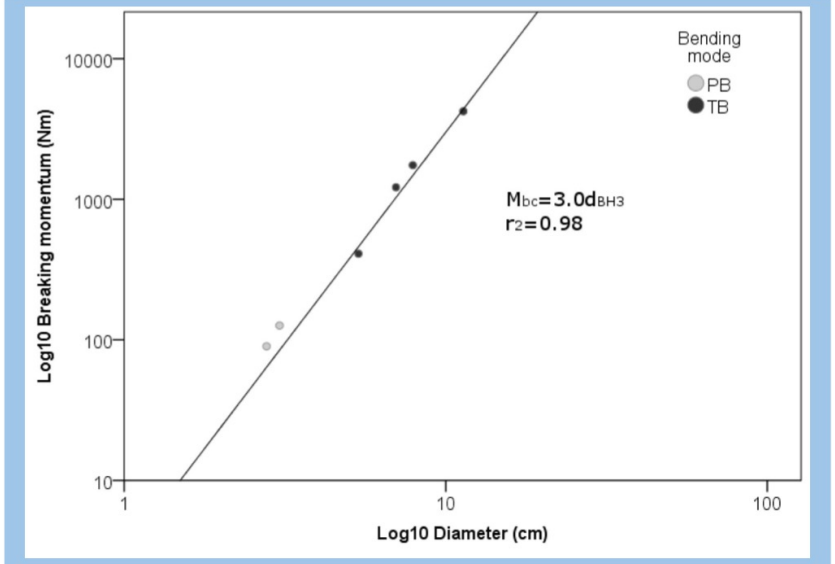

Politti, E., Bertoldi, W., Gurnell, A.M., Henshaw, A., 2017. Feedbacks between the riparian Salicaceae and hydrogeomorphic processes: A quantitative review. Earth-Science Rev. doi:10.1016/j.earscirev.2017.07.018

Kui, L., Stella, J.C., 2016. Fluvial sediment burial increases mortality of young riparian trees but induces compensatory growth response in survivors. For. Ecol. Manage. 366, 32–40.

Tanaka, N., Yagisawa, J., 2009. Effects of tree characteristics and substrate condition on critical breaking moment of trees due to heavy flooding. Landsc. Ecol. Eng. 5, 59–70.

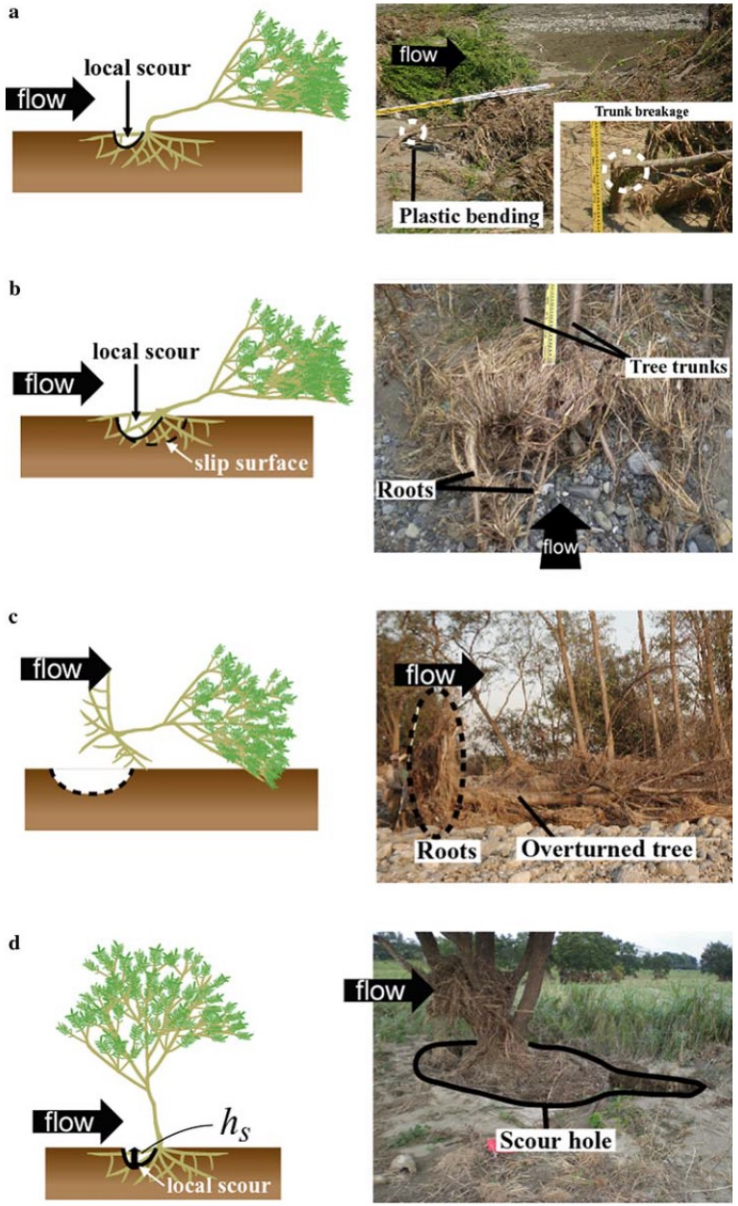

Wood logs resistance to pullout (early growth stages)

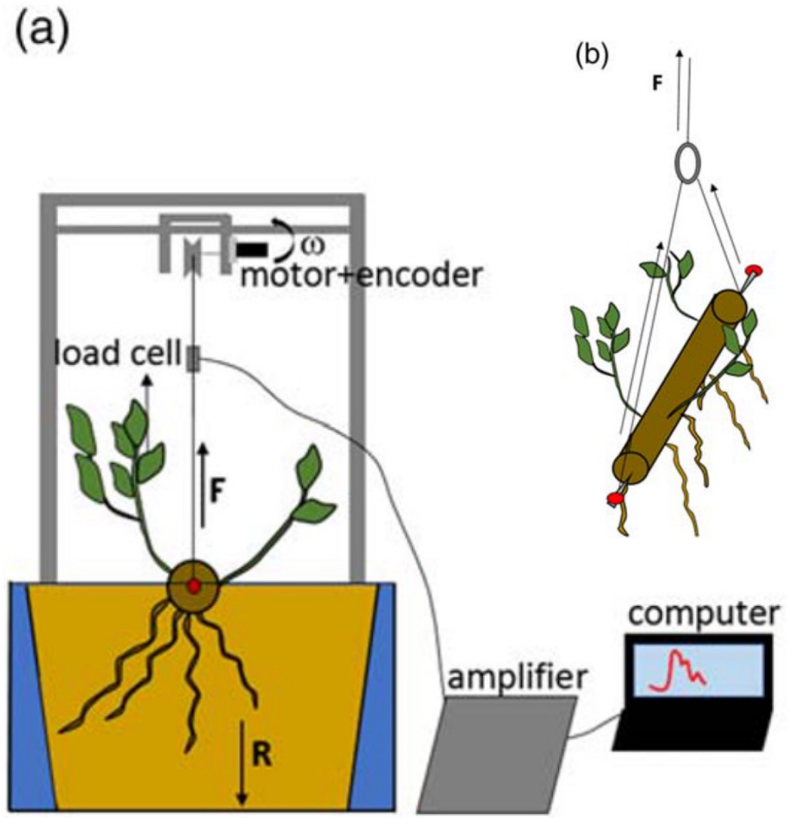

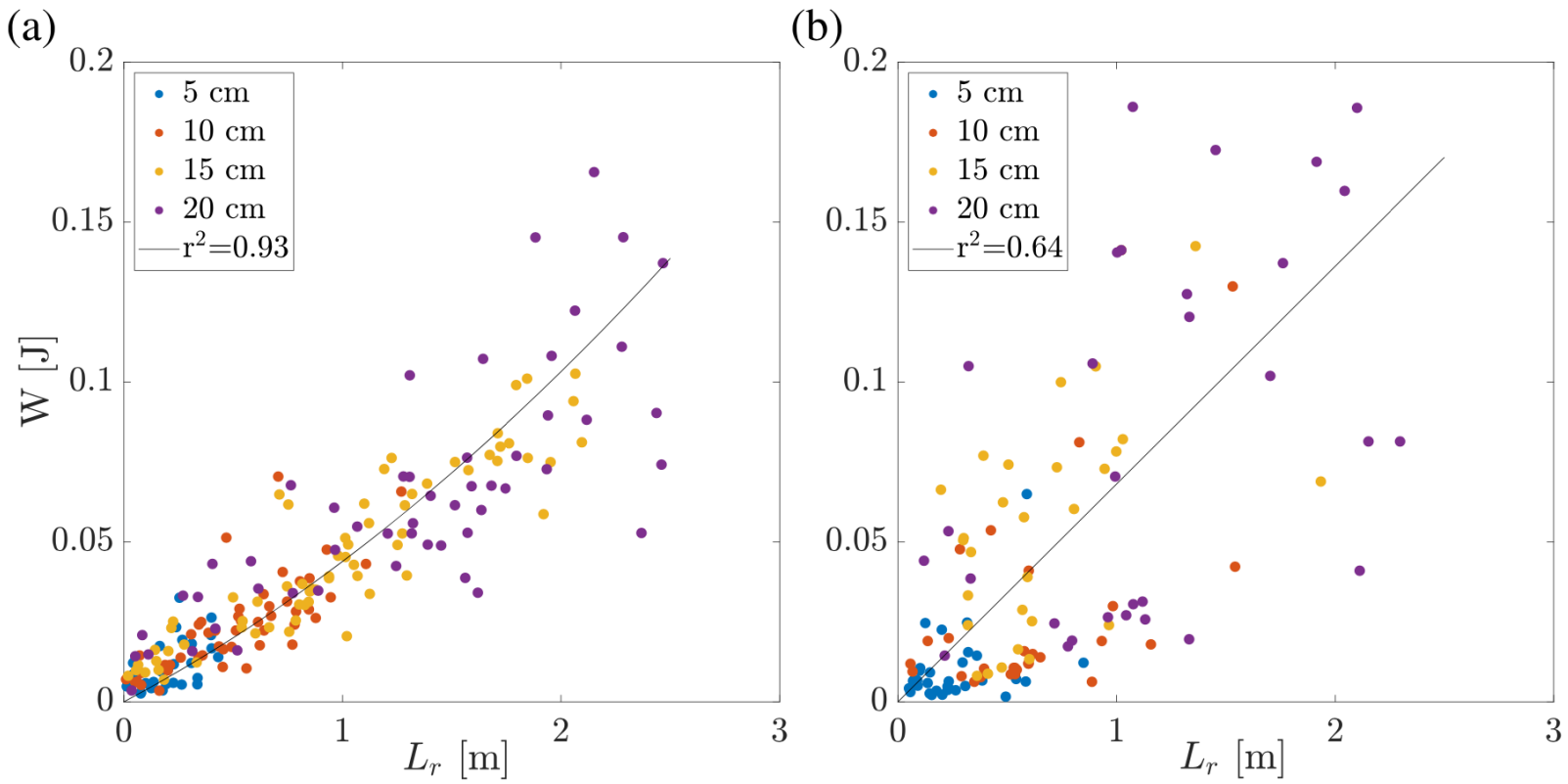

Sediment stabilisation by roots

Progress in Physical Geography 29, 2 (2005) pp. 189–217

Impact of plant roots on the resistance of soils to erosion by water: a review

G. Gyssels[1], J. Poesen[1,*], E. Bochet[2] and Y. Li[3]

[1]Physical and Regional Geography Research Group, K.U. Leuven, Redingenstraat 16, 3000, Leuven, Belgium
[2]Centro de Investigaciones sobre Desertificación (CSIC), Universitat València, Spain
[3]Institute of Agricultural Environment and Sustainable Development, Chinese Academy of Agricultural Sciences, Beijing, China

Abstract: Vegetation controls soil erosion rates significantly. The decrease of water erosion rates with increasing vegetation cover is exponential. This review reveals that the decrease in water erosion rates with increasing root mass is also exponential, according to the equation $SEP = e^{-b\,RP}$ where SEP is a soil erosion parameter (e.g., interrill or rill erosion rates relative to erosion rates of bare topsoils without roots), RP is a root parameter (e.g., root density or root length density) and b is a constant that indicates the effectiveness of the plant roots in reducing soil erosion rates. Whatever rooting parameter is used, for splash erosion b equals zero. For interrill erosion the average b-value is 0.1195 when root density (kg m^{-3}) is used as root parameter, and 0.0022 when root length density (km m^{-3}) is used. For rill erosion these average b-values are 0.5930 and 0.0460, respectively. The similarity of this equation for root effects with the equation for vegetation cover effects is striking, but it is yet impossible to determine which plant element has the highest impact in reducing soil losses, due to incomparable units. Moreover, all the studies on vegetation cover effects attribute soil loss reduction to the above-ground biomass only, whereas in reality this reduction results from the combined effects of roots and canopy cover. Based on an analysis of available data it can be concluded that for splash and interrill erosion vegetation cover is the most important vegetation parameter, whereas for rill and ephemeral gully erosion plant roots are at least as important as vegetation cover.

Key words: erosion models, plant roots, soil erosion, vegetation.

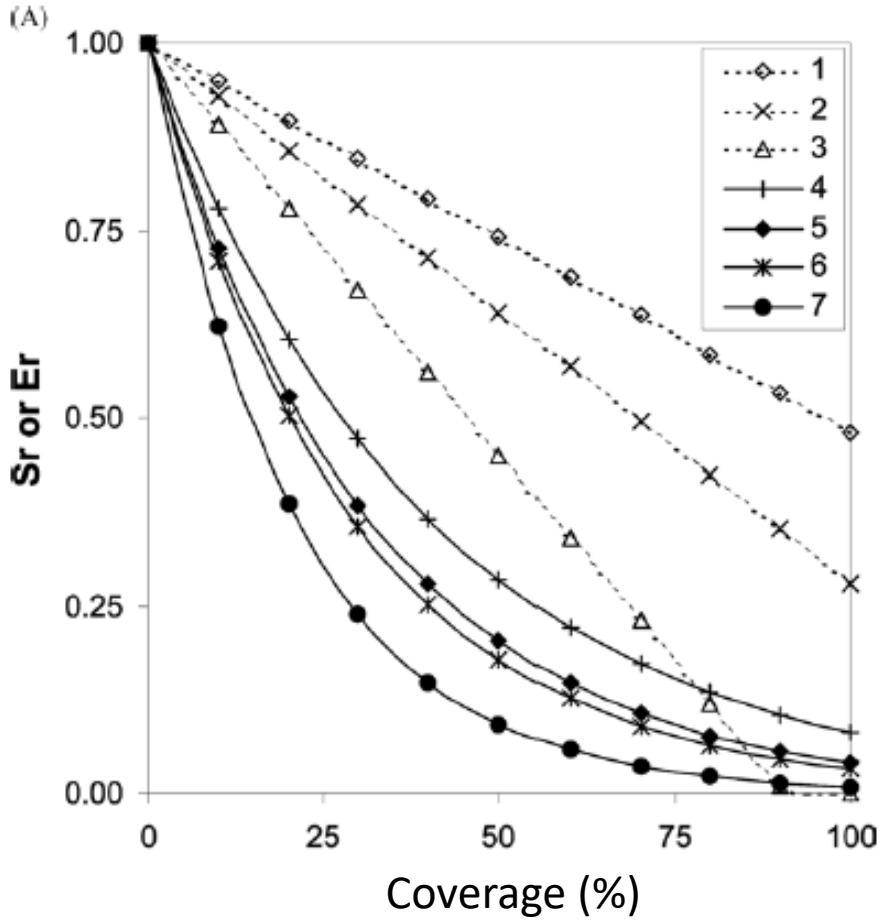

Empirical models based on modified Mohr-Coulomb equation

Additional cohesion due to roots

Water pore pressure

$$S = (C' + Cr) + (\sigma - \mu) \tan \phi'$$

Gray and Leiser, 1982

Total tensile root strength

$$Cr = T_r(A_r/A)\,(\cos \beta \tan \phi' + \sin \beta)$$

Wu et al., Can. Geotech. J., 1979

Shear distorsion from vertical

$$\approx$$

$$Cr = 1.2\, T_r(A_r/A)$$

Additional strength depends only on the amount of roots and their strength

Model limitations:

- Roots are assumed to be perpendicular to the slip plane (quite OK, lab exp shows that this compares to randomly oriented roots)
- Full tensile strength of all the roots is mobilized as the soils shears (disagreement with exps by Pollen et al., Wat. Sci. Appl. Ser., 2004)
- Roots are well anchored and do not pullout when tensioned (disagreement with exps, two main failure mechanisms are indeed pullout and/or rupture
- If failure occurs, then all roots break at the same time (disagreement with observations)

The fiber-bundle (Riproot) model

(Pollen-Bankhead and Simon, WRR, 2005)

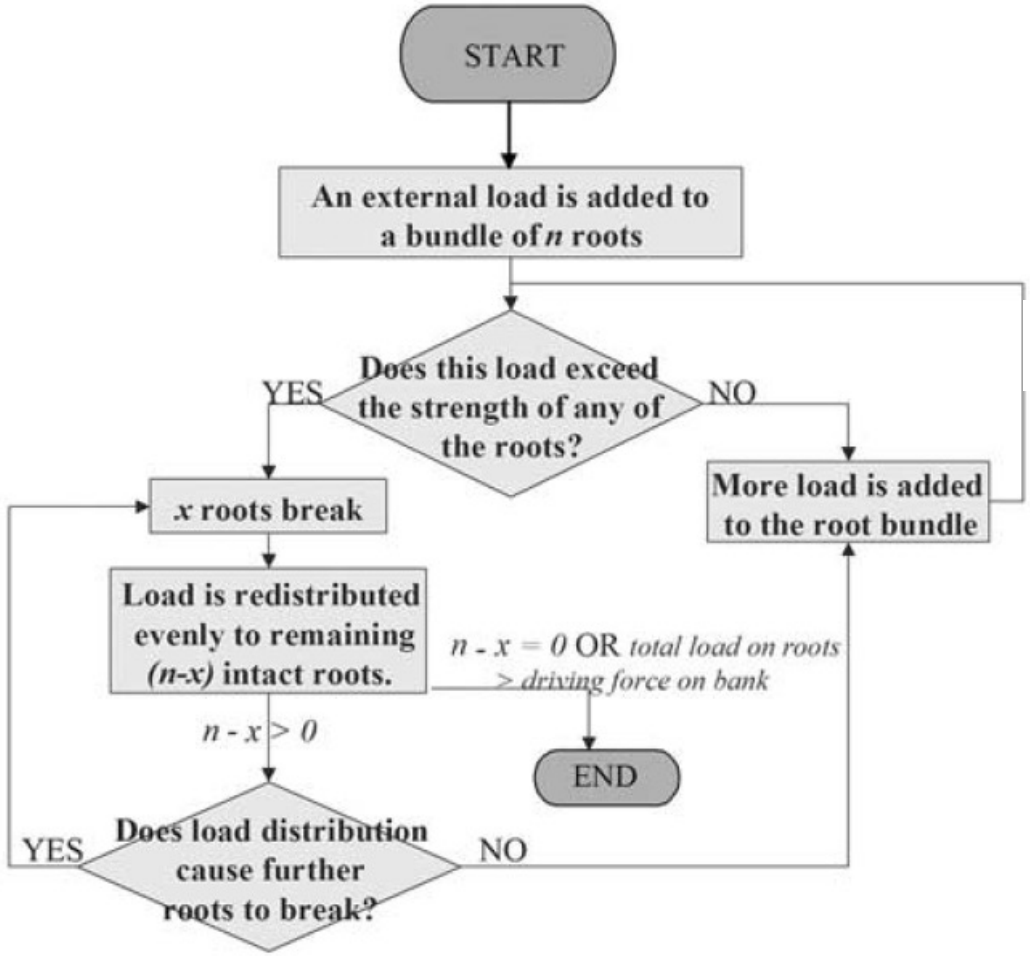

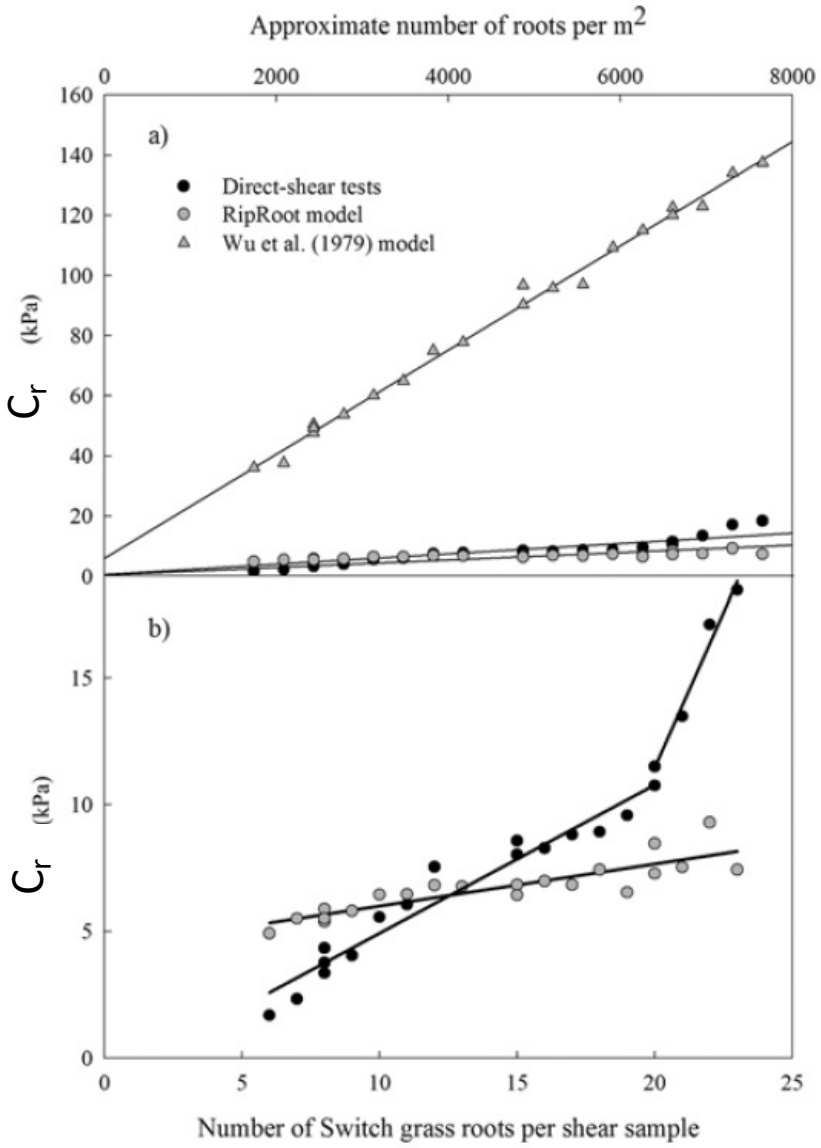

After Pollen and Simon, WRR, 2005

Pollen, Catena, 2006

BSTEM model to back calculate roots added “cohesion”

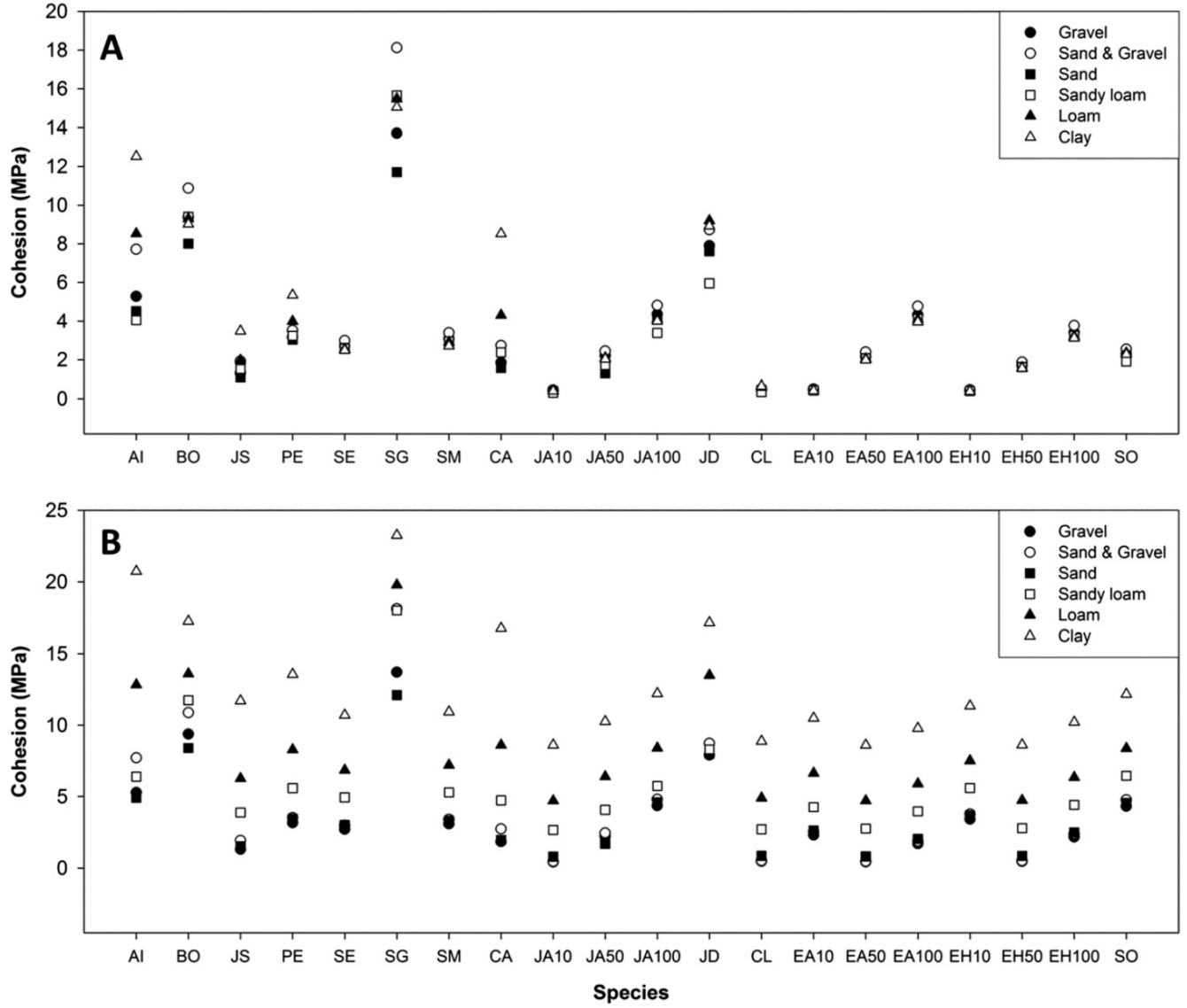

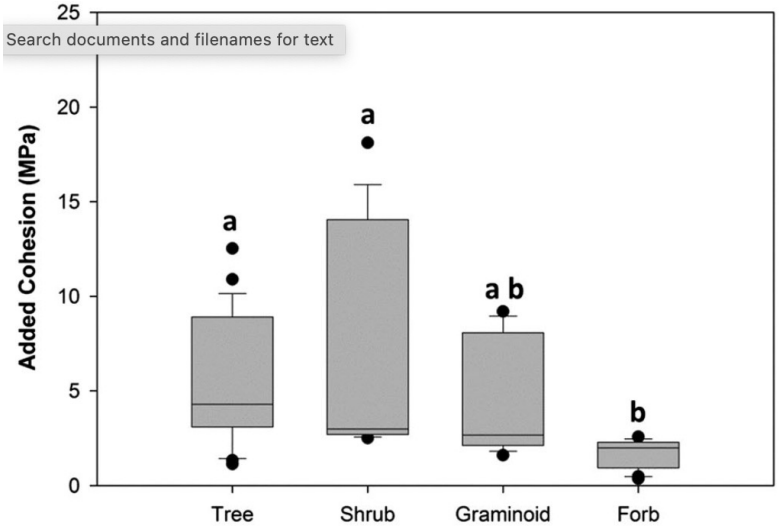

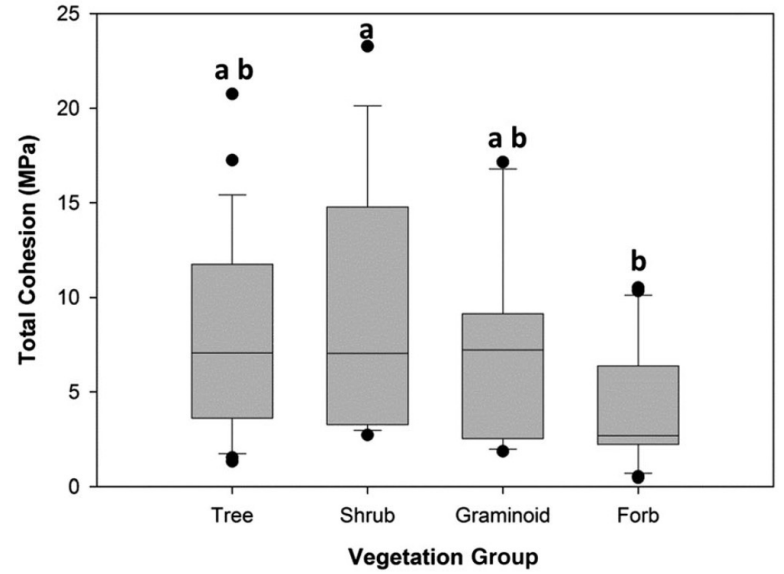

Sediment stabilisation from field experiments

Main idea: to compare scouring around and within low flow-blockage canopy (LFBC) plots
(Pasquale and Perona, River Flow 2014)

HYPOTHESES:
- Homogeneous grain size distribution;
- Homogeneous erosion at the cell scale;
- Average hydrodynamics conditions across the cell transect (no plot effects)

$$\Delta Q_s^{(e)} = \frac{\Delta V_m^{(e)}(1-\lambda)}{\Delta t^*} \qquad q_s^{(e)} = \frac{\Delta Q_s^{(e)}}{L_{cell}} \qquad q_s^{(e)} = 8\sqrt{(G-1)\,g d_{50}^3}\,(\tau^* - \tau_c^*)^{3/2}$$

$$\Delta Q_s^{(i)} = \frac{\Delta V_{plot}^{(i)}(1-\lambda)}{\Delta t^*} \qquad q_s^{(i)} = \frac{\Delta Q_s^{(i)}}{L_{cell}} \qquad \rightarrow \tau_{eq}^* = \left[\frac{1}{8\sqrt{(G-1)\,g d_{50}^3}} q_s^{(e)}\right]^{2/3} + \tau_c^*$$

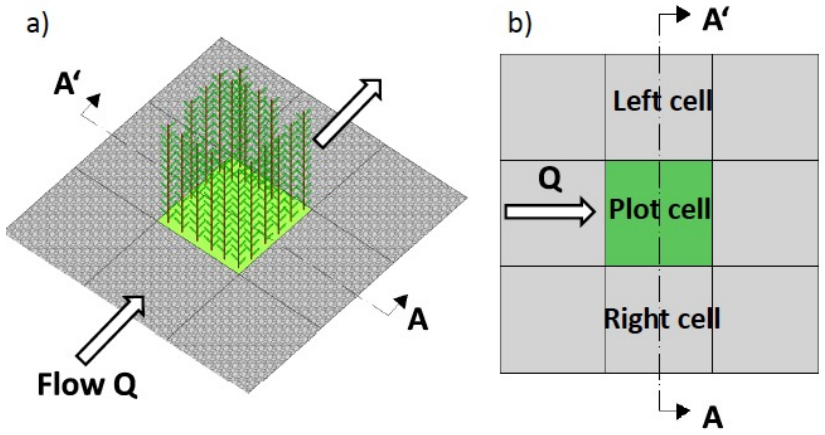

Low Flow Blockage Canopy (Rominger & Nepf, 2011)
$L_0 \approx 13$ m >> 2 m
→ negligible effect on hydrodynamics

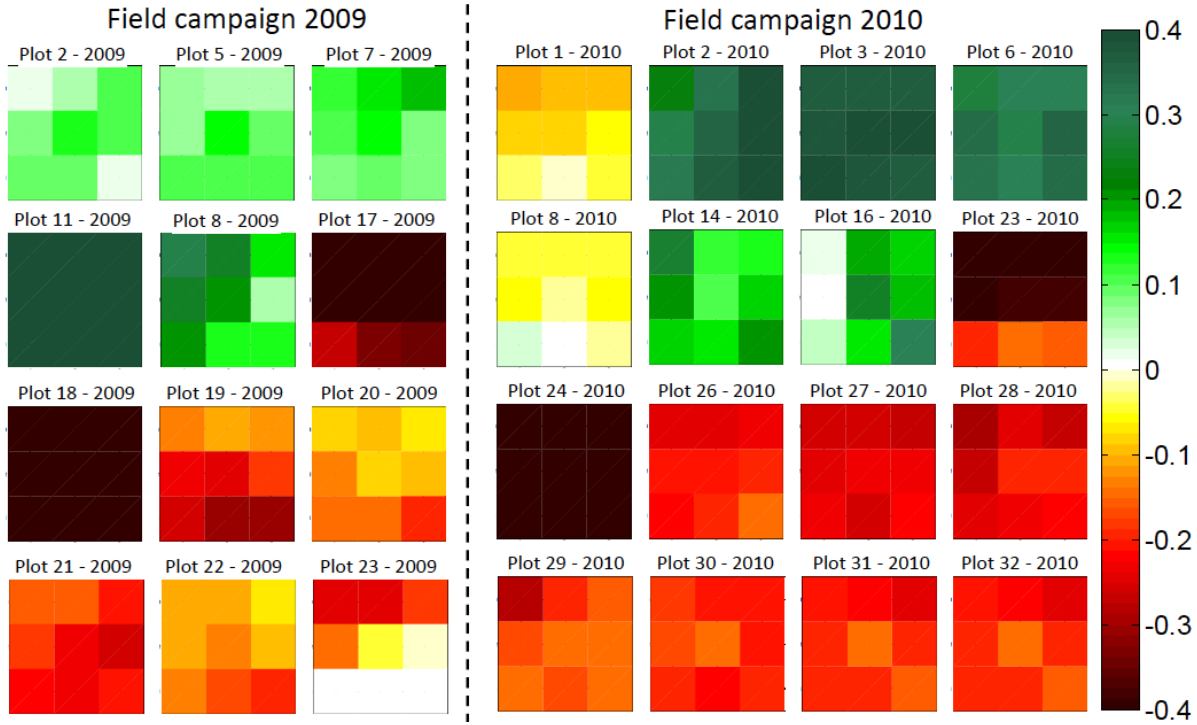

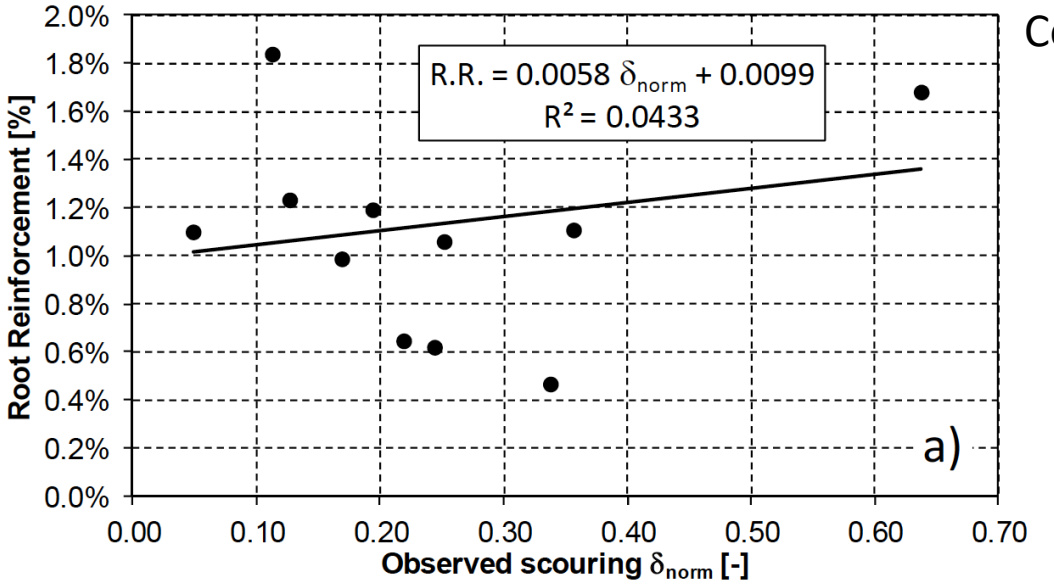

Correlation with scouring

Reinforcement depends on vertical root density distribution

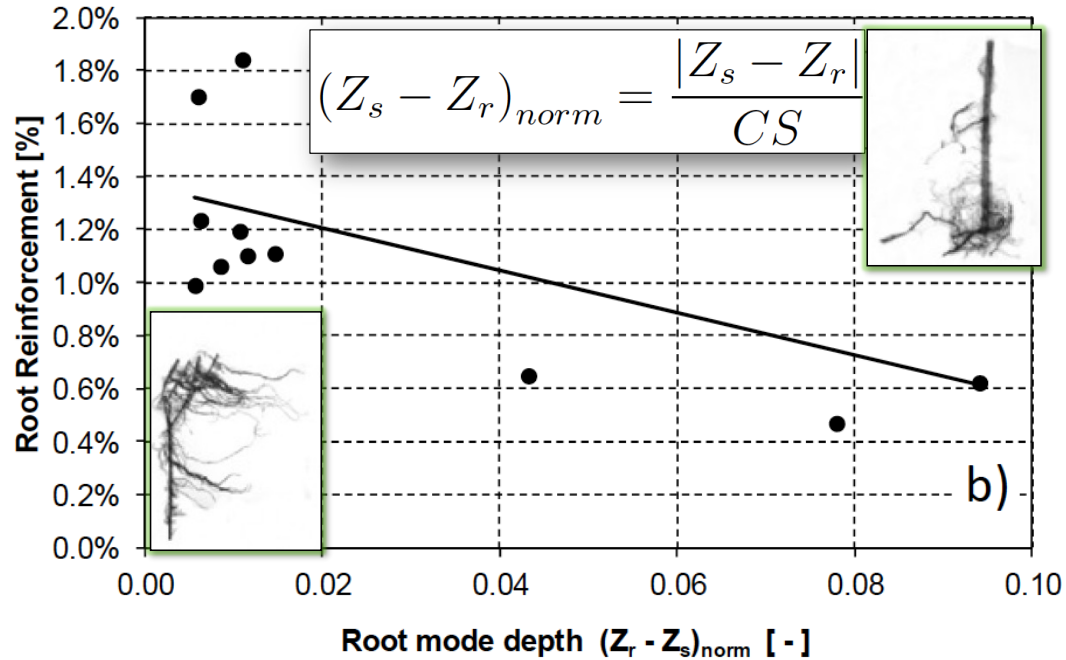

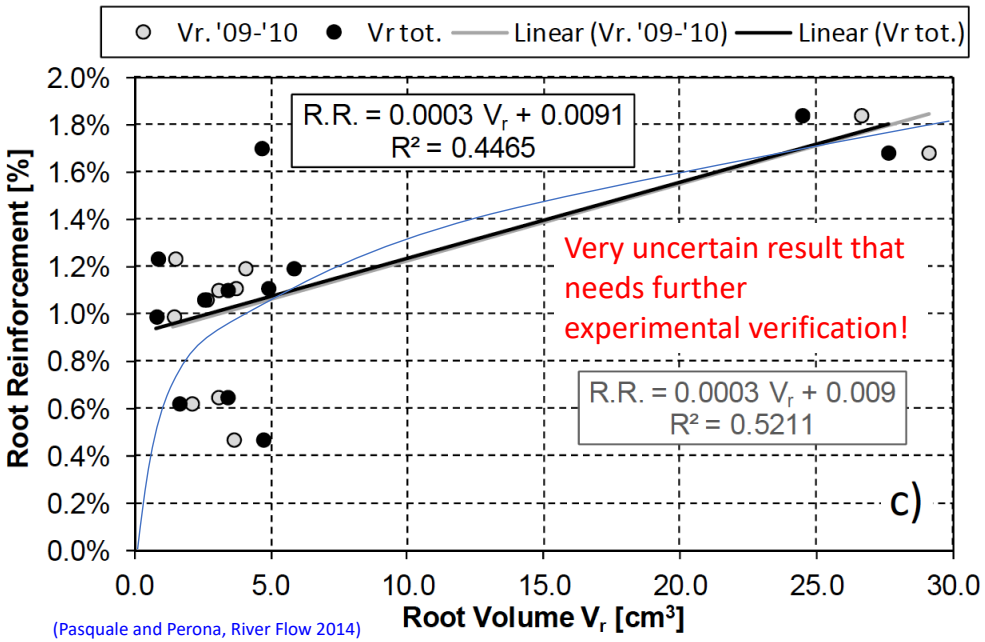

(Pasquale and Perona, River Flow 2014)

Reinforcement depends on root volume